USGS
science for a changing world

In cooperation with the
Michigan Department of Environmental Quality

Predicting Water Quality by Relating Secchi-Disk Transparency and Chlorophyll *a* Measurements to Satellite Imagery for Michigan Inland Lakes, August 2002

Scientific Investigations Report 2004-5086

U.S. Department of the Interior
U.S. Geological Survey

Cover Photograph. Lake Lansing, Ingham County, Michigan. (Photograph by L.M. Fuller, U.S. Geological Survey, August 2004.)

Predicting Water Quality by Relating Secchi-Disk Transparency and Chlorophyll *a* Measurements to Satellite Imagery for Michigan Inland Lakes, August 2002

By L.M. Fuller, S.S. Aichele, and R.J. Minnerick

Prepared in cooperation with the
Michigan Department of Environmental Quality

Scientific Investigations Report 2004-5086

U.S. Department of the Interior
U.S. Geological Survey

U.S. Department of the Interior
Gale A. Norton, Secretary

U.S. Geological Survey
Charles G. Groat, Director

U.S. Geological Survey, Reston, Virginia: 2004

For sale by U.S. Geological Survey, Information Services
Box 25286, Denver Federal Center
Denver, CO 80225

For more information about the USGS and its products:
Telephone: 1-888-ASK-USGS
World Wide Web: http://www.usgs.gov/

Suggested citation:
Fuller, L.M., Aichele, S.S., and Minnerick, R.J., 2004, Predicting water quality by relating secchi-disk transparency and chlorophyll *a* measurements to satellite imagery for Michigan inland lakes, August 2002: U.S. Geological Survey Scientific Investigations Report 2004-5086, 25 p.

Contents

Figures

Tables

Conversion Factors and Abbreviations

Multiply	By	To obtain
	Length	
foot (ft)	0.3048	meter (m)
mile (mi)	1.609	kilometer (km)
kilometer (km)	0.6214	mile (mi)
	Area	
acre	0.001562	square mile (mi^2)
acre	0.4047	hectare (ha)
micrometer (µm)	0.001	millimeter (mm)
	Concentration	
micrograms per liter (µg/L)	0.001	milligrams per liter (mg/L)

Abbreviated water-quality units used in this report: Chemical concentrations for Chlorophyll *a* and phosphorus are given in micrograms per liter (µg/L). Micrograms per liter is a unit expressing the concentration of chemical constituents in solution as a weight (micrograms) of solute per unit volume (liter) of water.

Miscellaneous Abbreviations

USGS	U.S. Geological Survey
MDEQ	Michigan Department of Environmental Quality
LWQA	Lake Water Quality Assessment program
CLMP	Cooperative Lakes Monitoring Program
SDT	Secchi-disk transparency
Chl-*a*	Chlorophyll *a*
AOI	Area of Interest

Predicting Water Quality by Relating Secchi-Disk Transparency and Chlorophyll *a* Measurements to Satellite Imagery for Michigan Inland Lakes, August 2002

By L.M. Fuller, S.S. Aichele, R.J. Minnerick

Abstract

Inland lakes are an important economic and environmental resource for Michigan. The U.S. Geological Survey and the Michigan Department of Environmental Quality have been cooperatively monitoring the quality of selected lakes in Michigan through the Lake Water Quality Assessment program. Through this program, approximately 730 of Michigan's 11,000 inland lakes will be monitored once during this 15-year study. Targeted lakes will be sampled during spring turnover and again in late summer to characterize water quality. Because more extensive and more frequent sampling is not economically feasible in the Lake Water Quality Assessment program, the U.S. Geological Survey and Michigan Department of Environmental Quality investigate the use of satellite imagery as a means of estimating water quality in unsampled lakes. Satellite imagery has been successfully used in Minnesota, Wisconsin, and elsewhere to compute the trophic state of inland lakes from predicted secchi-disk measurements. Previous attempts of this kind in Michigan resulted in a poorer fit between observed and predicted data than was found for Minnesota or Wisconsin. This study tested whether estimates could be improved by using atmospherically corrected satellite imagery, whether a more appropriate regression model could be obtained for Michigan, and whether chlorophyll *a* concentrations could be reliably predicted from satellite imagery in order to compute trophic state of inland lakes. Although the atmospheric-correction did not significantly improve estimates of lake-water quality, a new regression equation was identified that consistently yielded better results than an equation obtained from the literature. A stepwise regression was used to determine an equation that accurately predicts chlorophyll *a* concentrations in northern Lower Michigan.

Introduction

The State of Michigan has more than 11,000 inland lakes; approximately 3,500 of these lakes are greater than 25 acres in size. Nearly all of these lakes greater than 25 acres have developed communities with permanent residences or vacation homes. The general public has access to launches or beaches at about 1,300 lakes in Michigan. Recreational value, property values, and ecological value are all closely related to the quality of water in these inland lakes (Krysel and others, 2003). Tourism in Michigan, much of which involves recreation at inland lakes, accounts for nearly $15 billion of economic activity each year (Stynes, 2002). Thus, inland lakes are important economic and ecological resources to Michigan.

The U.S. Geological Survey (USGS) and the Michigan Department of Environmental Quality (MDEQ) have been cooperatively monitoring the quality of inland lakes in Michigan through the Lake Water Quality Assessment (LWQA) monitoring program funded by the Clean Michigan Initiative. Through this program, the USGS will sample approximately 730 lakes over 25 acres in size with public access during a 15-year period. The 730 lakes are grouped into 45 major watershed management units. In a given year, a set of 7 to 10 of the 45 major watershed management units is chosen for sampling and lakes to be sampled are randomly selected from this set. After 5 years, at least some lakes in each of the 45 major watershed management units will have been sampled. This 5-year rotation will continue until year 2015, when all targeted 730 lakes have been sampled once. In addition, each year the MDEQ will provide data from their Cooperative Lakes Monitoring Program (CLMP), which is a volunteer network monitoring more than 200 lakes. Data from those two sampling networks are used to characterize baseline water quality and compute trophic state of monitored inland lakes.

Measured water-quality characteristics of inland lakes are critical factors in determining their recreational use, habitat and species diversity, and the economic return from the tourism industry. The USGS and the MDEQ monitor many inland lakes, but it is not economically feasible to monitor the quality of all 11,000 inland lakes in Michigan by use of conventional sampling techniques. Knowledge of the biological productivity of unsampled inland lakes is needed to assist resource managers in their efforts to help protect and manage the quality in all of Michigan's inland lakes.

Satellite imagery has been successfully used in Minnesota (Olmanson and others, 2001), Wisconsin (Batzli, 2003), and elsewhere (Baban, 1993; Dekker and Peters, 1993; Mayo and others 1995; Giardino and others, 2001) to estimate water quality for unsampled inland lakes. In previous studies in Michigan (Nelson and others, 2002; Wianwang, 2002) researchers attempted to use existing models for relating satellite imagery to specific water-quality variables; however, they were unable to obtain as high a coefficient of determination (R^2), which indicates the strength of a statistical relation, as previous studies in Minnesota and Wisconsin. A better method to predict trophic characteristics from satellite imagery would increase the knowledge every year about more of Michigan's inland lakes.

Purpose and Scope

The purpose of this report is to describe the methods and techniques used to develop estimates of Michigan lake-water quality on the basis of satellite images. Specifically, this report presents a brief overview of the conceptual basis for predicting trophic state on the basis of satellite images, describes methods used to develop a new alternative regression model for predicting secchi-disk transparency, and offers a new regression equation for predicting chlorophyll *a* concentrations in northern Lower Michigan. These two measures can further be used to estimate the trophic state of Michigan inland lakes.

Background

Naumann (1919) proposed a classification of lake-water quality ranging from oligotrophic (low phytoplankton populations and low primary productivity) to eutrophic (high phytoplankton populations and high primary productivity). Carlson (1977) proposed to quantify the trophic state by using a Trophic State Index (TSI), which can be used to group lakes into basic classes of oligotrophic, mesotrophic, eutrophic, and hypereutrophic. The natural progression of a lake from oligotrophic to eutrophic can be computed from measures of total phosphorus (TP), secchi-disk transparency (SDT), and chlorophyll *a* (Chl-*a*).

TP is measured directly by sampling and chemical analysis. SDT is a commonly used, low-cost technique that measures water clarity (Specifically, a black and white disk is lowered into the lake until it can no longer be seen). Water clarity is related to the quantity of phytoplankton in the water, although non-algal turbidity and tannic acids also can reduce water clarity. Chl-*a* measurements correlate with the concentration of phytoplankton within a given volume of lake water and are not affected by sediment or acids in the water. The formulas for computing TSI values are (Carlson, 1977):

$$TSI_{TP} = 14.41 * ln\ TP(milligrams\ per\ liter) + 4.15, \quad (1)$$

$$TSI_{SDT} = 60 - 14.41 * ln\ SDT(meters), \quad (2)$$

and

$$TSI_{CHL-a} = 9.81 * ln\ Chl-a(milligrams\ per\ liter) + 30.6 \cdot \quad (3)$$

The range of TSI values and how each measure is classified into oligotrophic, mesotrophic, eutrophic, and hypereutrophic is listed in table 1.

Typically, computing TSI values for a single lake using all three formulas should yield similar results. Increasing the phosphorus concentration generally results in increased phytoplankton concentration, which results in reduced water clarity. Yet at specific times of the year, results from the three formulas may not be congruous because of phosphorus nutrient uptake by macrophytes. Therefore, substantial amounts of macrophytes in a lake may alter the relation of the three TSI values. Of the three measures, SDT and Chl-*a* concentration have been quantified by use of satellite imagery techniques (Mayo and others, 1995; Zilioli and Brivio, 1997; Cox and others, 1998; Kloiber and others, 2000; Giardino and others, 2001; Kloiber and others, 2002).

Table 1. Lake trophic states and classification ranges for trophic state index, total phosphorus, secchi-disk transparency, and chlorophyll *a*.

[Based on Michigan Department of Environmental Quality report (1982) and modified by the State of Michigan to account for regional characteristics. TSI, Trophic State Index; SDT, secchi-disk transparency; Chl-*a*, Chlorophyll *a*; TP, Total Phosphorus; ft, feet; µg/L, micrograms per liter]

Lake trophic condition	Carlson TSI	SDT (ft)	Chl-*a* (µg/L)	TP (µg/L)
Oligotrophic	<38	>15	<2.2	<10
Mesotrophic	38–48	7.5–15	2.2–6	10–20
Eutrophic	49–61	3–7.4	6.1–22	20.1–50
Hypereutrophic	>61	<3	>22	>50

Satellites have been used to predict water characteristics since the 1970s. For example, the National Aeronautics Space Administration (NASA) Earth Resources Technology Satellite (ERTS-1) was used to determine an algal bloom in Lake Erie in 1972 (Strong, 1974). NASA's Landsat satellite series improved the spatial, spectral, and radiometrical resolutions allowing more water-quality parameters to be studied. The idea to relate SDT to satellite imagery started in the late 1970s and studies involving Chl-*a*, turbidity, and other water-quality characteristics soon followed (Scarpace and others, 1979; Lillesand and others, 1983; Verdin, 1985; Lathrop and Lillesand, 1986; Dekker and Peters, 1993; Mayo and others, 1995; Zilioli and Brivio, 1997). Landsat bands 1 through 4 signifying the visible and near infrared portions of the electromagnetic spectrum, were found to correlate well with water-quality characteristics (Lathrop and Lillesand, 1986). However, Lathrop (1992) found it difficult to use the same regression equation to characterize the water quality of different lakes. Recent studies found that, with improved methods, it was possible to predict water quality for unsampled lakes by use of regression equations relating existing measurements to remotely sensed data (Pulliainen and others, 2001; Kloiber and others, 2002; Thiemann and Kaufmann, 2002). These most recent studies form the basis for this project.

Imagery used in this study was collected by the Landsat 7 Enhanced Thematic Mapper Plus (ETM+) satellite launched in 1999 by NASA. The satellite orbits at an altitude of approximately 705 km with a sun-synchronous 98-degree inclination and a descending equatorial crossing time of 10:00 a.m. (Williams, 2003). Every 16 days, the satellite will repeat coverage for each scene coinciding with the Landsat Worldwide Reference System (WRS), which records satellite scenes into a grid reference system made up of 233 paths and 248 rows. The Landsat 7 ETM+ sensor collects information in nine bands, distinct portions of the electromagnetic spectrum. Bands 1, 2, 3, 4, and 8 are sensed within a spectral range between 0.4 and 1 µm. Bands 1, 2, and 3 correspond to the visible spectrum of blue, green, and red, and band 4 is infrared; together, these bands span the spectral range of 0.45 to 0.90 µm. Bands 5 and 7 are short-wavelength infrared bands sensed within a spectral range between 1 and 3 µm. Bands 6a and 6b are thermal long wavelengths sensed within a spectral range between 8 and 12 µm. Band 8 is the panchromatic band that combines bands 2, 3, and 4 with a spectral range of 0.52 to 0.90 µm (Williams, 2003). Data are reported in digital numbers as 8-bit integers, ranging from 1 to 256.

Several distortion factors affect satellite imagery. These factors include geometric distortions that are the result of small imprecisions in maneuvering the sensor; radiometric distortions that arise from small differences in the calibration of the sensor and geometry of the earth, sun, and satellite; and atmospheric distortions that arise from scattering of light by moisture and particulates in the atmosphere. However, procedures have been developed to help correct for these factors. Geometric and radiometric corrections can be made with little or no field data. However, most studies of this scope suggest that the imagery should be geometrically, radiometrically, and atmospherically corrected (Brivio and others, 2001; Zilioli and Brivio, 1997; Kloiber and others, 2002).

A variety of equations relating satellite imagery to STD have been tested in different settings and with different sensors. Researchers that use imagery from the Landsat 7 ETM+ satellite (Kloiber and others, 2002) have generally used the following equation:

$$ln(SDT) = a(band1/band3) + b(band1) + c . \quad (4)$$

The variables *a*, *b*, and *c* are empirically derived coefficients from the regression equation.

Nelson and others (2002) used raw digital numbers from the images and the regression equation identified in Kloiber and others (2002) to estimate SDT for lakes in Lower Michigan. Kloiber and others (2002) reported predictions with R^2 values between 0.72 and 0.93. Nelson and others (2002) achieved an R^2 of only 0.43 for Landsat ETM+ scenes in path 21, rows 29, 30, and 31. Wiangwang (2002) used the same imagery and field data as Nelson and others (2002) but radiometrically corrected the images before determining regression equations. This type of correction is termed "Top of Atmosphere" (TOA) reflectance because, although it accounts for differences in illumination angle and sensor performance, it does not adjust for haze or diffusion within the atmosphere. The R^2 value using SDT and Landsat 7 ETM+ TOA corrected imagery for path 21, rows 29, 30, and 31 was 0.558 (Wiangwong, 2002). This result suggests that a full atmospheric-correction of the imagery could in theory further improve the R^2 values. The combination of all of these techniques in the same case study should improve the regression equations, and thus lead to better methodology to estimate water quality from satellite imagery.

Study Area

The study area was determined by the location of LWQA sampling planned for the 2002 water year (the 2002 water year was a portion of the inland lakes chosen to be sampled from 10 out of the 45 basins in Michigan). Most measurements fell within five Landsat 7 ETM+ satellite scenes covering the majority of Lower Michigan. The locations of the satellite scenes and the lakes with collected SDT measurements within a window of plus or minus 7 days of the imagery acquisition, are shown in figure 1.

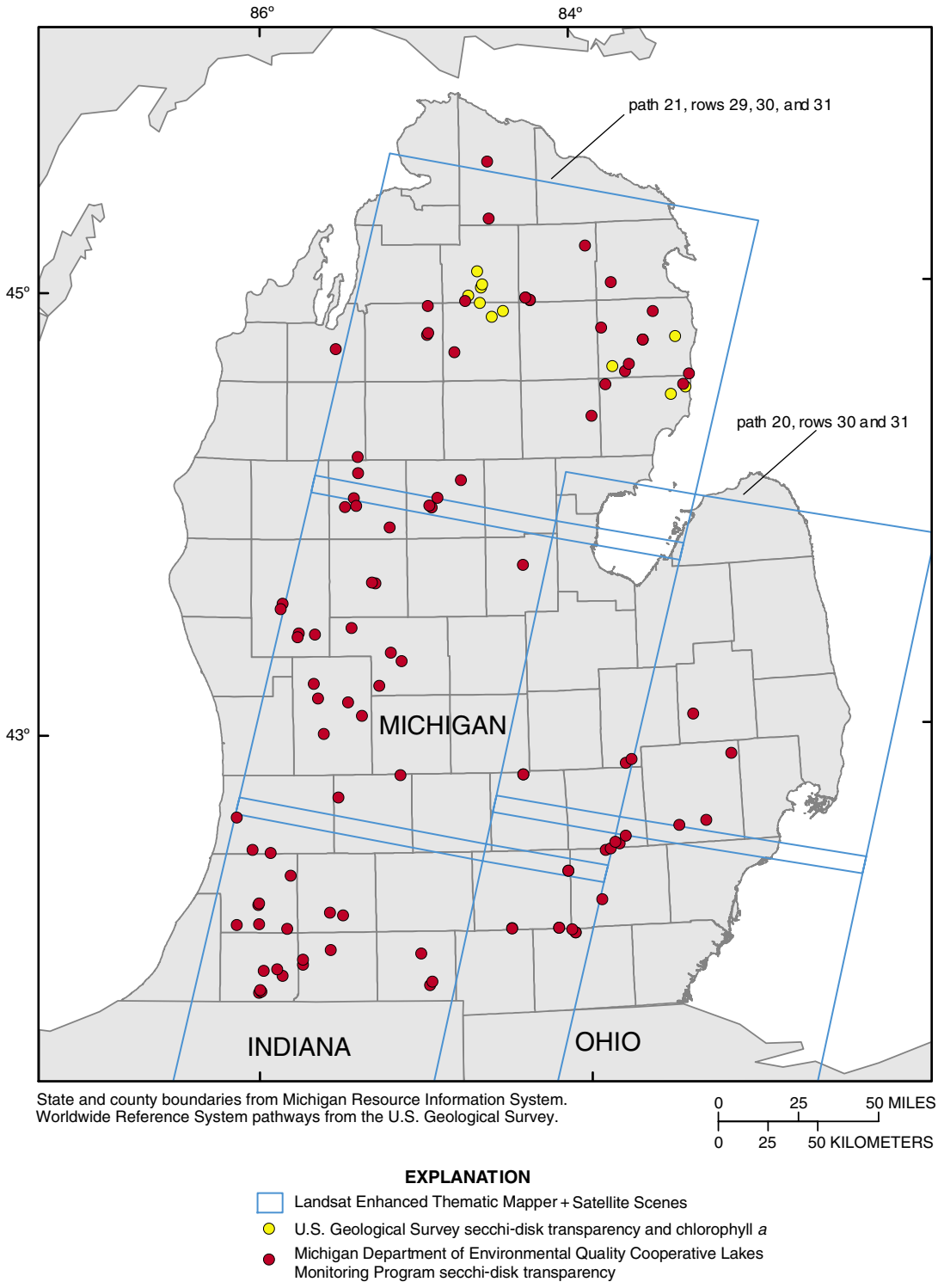

Figure 1. Secchi-disk transparency and chlorophyll *a* sample locations, Michigan, August 2002.

Methods

The general process to predict SDT and Chl-*a* measurements from satellite imagery involves several steps. First, field data must be obtained and digitized. Second, cloud-free satellite imagery from approximately the same date as the field data collection must be obtained. Third, the imagery must be corrected to compensate for geometric, radiometric, and atmospheric distortions in the imagery. Fourth, the field data must be compared to the imagery through the creation of Areas of Interest (AOI) within the satellite image. Fifth, a regression model must be developed for each scene to relate the field data to the spectral data collected in each AOI. Finally, the regression equation must be applied to all lakes over 25 acres in the satellite scene, to predict the water-quality characteristics at unmeasured locations.

Field Data Collection and Preprocessing

USGS scientists and community volunteers from the CLMP routinely measure SDT in various lakes in Michigan. A secchi disk is a common tool for measuring the overall clarity of water. The Secchi disk is an 8-in. diameter circular disk painted black and white in alternating quadrants. The disk is lowered into the water, and the depth at which the disk is no longer visible is called the secchi depth. Chl-*a*, TP, several forms of nitrogen, and major ions are also measured at USGS sample sites. Samples from both the CLMP and USGS were used from the months of August and September 2002. This late-summer index period, when a lake is at the maximum biological productivity, was found to be the best period for relating SDT and Chl-*a* samples to satellite imagery (Kloiber and others, 2000).

USGS measurements were referenced by coordinates obtained from the Global Positioning System (GPS) and were used to create a shapefile. A shapefile is the file format ArcGIS software uses to store the location, shape, and attribute information. The SDT measurements from CLMP were recorded on paper and did not include precise coordinates for the measurements; however, a bathymetric map for each lake marked in the approximate location for each measurement. With this information, another shapefile was made by manually digitizing the correct location for all data within the lakes.

Volunteer SDT measurements have been studied and proven to be comparable with those made by professionals (Canfield and others, 2002; Obrecht and others, 1998). However, careful consideration was involved in choosing which CLMP SDT measurements were used in this study. Only measurements that were clearly marked on attached bathymetric maps were digitized. Some volunteer data were excluded where multiple measurements were made in a single lake (only one measurement per lake was chosen within the deepest basin) and when the location of measurements could not be determined from the published bathymetric maps.

Only measurements collected within 7 days of an image acquisition date were used. This restriction was shown to produce the best results in predictive SDT models (Kloiber and others, 2002). The final exclusions for all measurements were dependent upon the satellite imagery. Measurements when clouds or cloud shadows covered the lake or measurement location were excluded. Clouds and shadows are limiting factors and are the reason imagery should be chosen on clear satellite overpass days. (For a summary of sample numbers per scene refer to table 4.)

Satellite Imagery Acquisition and Preprocessing

Five Landsat 7 ETM+ scenes were purchased from the Tropical Rain Forest Information Center, a member of NASA Federation of Earth Science Information Partners at the Center for Global Change and Earth Observations, Michigan State University. The scenes from path 20, rows 30 and 31, and path 21, rows 29, 30, and 31 were chosen because they had minimal cloud cover and were acquired closest to the dates when the measurements were collected. For reference, see figure 1, which depicts satellite scene locations with the placement of SDT and Chl-*a* measurements.

The data arrived with a geometric systematic correction, which helped ensure that the image cells would correspond to the data-collection points as closely as possible. The systematic correction refers to the type of geometric correction. “The end result is a geometrically rectified product free from distortions related to the sensor (e.g. jitter, view angle effects), satellite (e.g. attitude deviations from nominal), and earth (e.g. rotation, curvature)” (National Aeronautics Space Administration, 2003). However, the geometric correction did not use ground-control points to ensure complete geodetic accuracy, and NASA only claimed residual error to 250 m in flat terrain at sea level. When each image was compared with the Michigan transportation framework developed by the Michigan Center for Geographic Information, however, it was found to be accurate to within 2 cells, or about 60 m.

The satellite imagery was also radiometrically corrected by use of a radiative transfer model. Radiometric corrections are needed because the brightness of each pixel in a satellite image is “affected by sun angle, atmospheric interference, changes in detector response, and numerous other factors” (Kloiber and others, 2002). The atmospheric-correction method used was MODTRAN4, released by the Air Force Research Lab, Space Vehicles Directorate, in March 1999. This model is an atmospheric radiative transfer code and algorithm (Hoke, 1999).

Atmospheric-Correction

To test whether atmospherically correcting the imagery would achieve better fit regression equations, path 21, rows 29, 30, and 31 were atmospherically corrected. The atmospheric correction model MODTRAN4 (Hoke, 1999) was used. Each

satellite scene was run seven times through the model, keeping all parameters constant for each scene except the surface percent reflectance, which started at 0.1 and increased to 0.7. The different surface percent reflectances were used to construct regression equations that accounted for atmospheric scattering of both incoming solar radiation and outgoing reflected radiation. The results were equations describing the relation between reflected radiation and radiation measured at the sensor. These equations were then applied to their corresponding bands to atmospherically correct the imagery. The inputs are listed in table 2. The output slope and intercept coefficients for each band were used in an Erdas IMAGINE model (Erdas Inc, 2001) to build the equations to compute atmospherically corrected images. The equations take into account that shorter wavelengths, such as band 1, scatter more than longer wavelengths, such as band 5. The values for all bands generally increase with this correction, but band 1 shows the most increase and band 5, the least. Typical change between the TOA reflectance values and the resulting atmospheric-correction values for Lake Lansing in Ingham County are shown in figure 2.

Table 2. MODTRAN4 atmospheric-correction parameters and input.

[km, kilometers]

Parameter	Input
Surface percent reflectance	0.1 to 0.7
Atmospheric model	Midlatitude summer
Aerosol model	Rural extinction (default visibility = 23 km)
Season	Spring-summer
Visibility	23 km
Day of year	Dependent upon satellite scene
Latitude and longitude	Varied depending on center of satellite scene
Greenwich mean time of image acquisition	1430

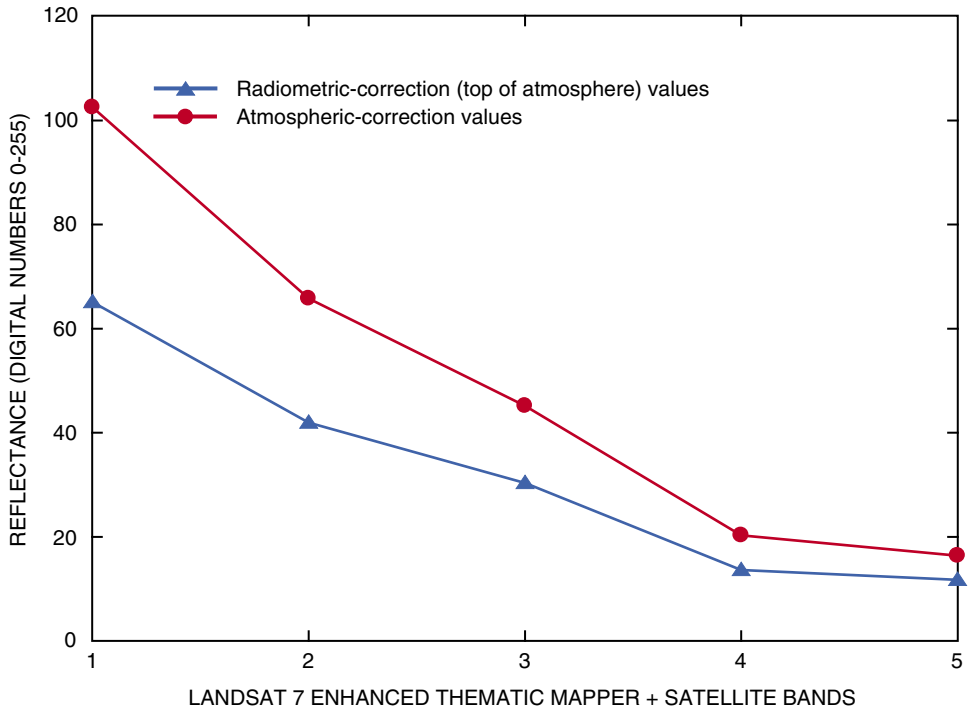

Figure 2. Radiometric-correction (top of atmosphere) reflectance values compared to atmospheric-correction values, Lake Lansing, Ingham County, Mich.

Relating Field Data to Satellite Imagery

Area of Interest Creation

The six shapefiles that were created corresponding to the SDT and Chl-*a* measurements for each scene were opened on top of the appropriate satellite scene in Erdas IMAGINE. Areas of Interest (AOIs) were digitized around the SDT measurements for five scenes, and Chl-*a* measurements for one scene. An area was drawn around each measurement to include pixels surrounding the measurements to help smooth radiometric noise. The AOI sizes depended on the size of the lake but were between the minimum of 8 pixels and the maximum of 1,000 pixels set by Olmanson and others (2001). The smallest AOI was 8 pixels, the mean was 12 pixels, and the maximum was 33 pixels.

Once all the AOIs were drawn around measurements within a satellite scene, each one was added to the signature file and the minimum, maximum, standard deviation, and mean value for each band within the AOI was computed. These results were then exported into a datafile format for further calculation. Results for the measurement values within the corresponding AOIs can be found in Appendix A.

Water-Only Imagery

A few steps were performed in Erdas IMAGINE to extract pixels in each image that would correspond to an inland lake greater than 25 acres. First, an unsupervised classification identified the water pixels (30-m cells). Next, the pixels were grouped into contiguous bodies of water to identify the inland lakes that were greater than 25 acres or 125 pixels. Finally, the pixels that corresponded to an inland lake greater than 25 acres were coded to a value of 1, with all other pixels coded to a no-data value to complete the water-only images.

Regression Equations and Tests of Significance for Secchi-Disk Transparency

In preparation for regression analysis, the band1/band3 ratio, the natural log of SDT (in meters) were computed. The data were then transferred into S-Plus 2000 (Data Analysis Products Division, 1999) for multiple regression calculations based on scene and type of measurement. (The combinations used in the regression equations are listed in table 3).

The equation developed by Kloiber and others (2000):

$$ln(SDT) = a(band1/band3) + b(band1) + c, \quad (5)$$

was applied to each TOA and atmospherically corrected scene. The variables *a*, *b*, and *c* were derived coefficients from the regression equation. In an effort to improve the goodness of fit for the model, various combinations of bands were tested. For the Kloiber (2000) equation, TOA and atmospherically corrected R^2 values were compared. A new, alternative equation also was developed during the project. For the new alternative equation,

$$ln(SDT) = a(band1) + b(band2) + c(band3) + d, \quad (6)$$

TOA and atmospherically corrected R^2 values were compared. To test whether there was a statistically significant difference between the R^2 values, Fisher's Transformation was used:

$$Z = (\{0.5*ln[(1+r_1)/(1-r_1)]\} - \{0.5*ln[(1+r_2)/(1-r_2)]\})/SQRT[1/(n-3)] \quad (7)$$

In the equation, r1 and r2 represent the two R^2 values that were being tested, ln refers to base *e* and *n* refers to the number of samples. The results of Fisher's Transformation had to surpass 1.96 for a 95-percent confidence interval. This test was also used to determine whether there was any difference between the two equations to compute TSI from the predicted natural log of SDT and to test whether there was any difference between using the TOA or atmospherically corrected scenes from path 21.

Stepwise Regression Equations for Chlorophyll *a*

To identify the best-fit regression equation for predicting Chl-*a*, a stepwise regression was used. In this process the natural log of measured Chl-*a* and various combinations of bands were used in four separate trials to determine the bands or combinations of bands with the best coefficients. For a list of the variables tested, refer to table 4.

Table 3. R^2 values and Fisher's Transformation significance tests used to compute trophic state index for Michigan's inland lakes from predicted secchi-disk transparency.

[ln, natural log; ETM+, Enhanced Thematic Mapper Plus; TOA, Radiometric-correction values of Top of Atmosphere Reflectance; ATM, Atmospheric-Correction; R^2, R Squared; Eq, equation; †, Not tested]

Equation 1	Independent variable: ln (secchi depth in meters)		
Secchi-disk transparency	**Dependent variables: band 1/band 3, and band 1**		
Landsat 7 ETM+ scenes	**Samples**	**TOA R^2**	**ATM R^2**
path 20, row 30	15	0.5075	†
path 20, row 31	13	.3003	†
path 21, row 29	28	.6640	0.6737
path 21, row 30	29	.7995	.7995
path 21, row 31	25	.6014	.6072

Equation 2	Independent variable: ln (secchi depth in meters)		
Secchi-disk transparency	**Dependent variables: band 1, band 2, band 3**		
Landsat 7 ETM+ scenes	**Samples**	**TOA R^2**	**ATM R^2**
path 20, row 30	15	0.7190	†
path 20, row 31	13	.6659	†
path 21, row 29	28	.7824	0.7875
path 21, row 30	29	.7964	.7964
path 21, row 31	25	.6058	.6101

Fisher's Transformation: R^2 Equation 1 and Equation 2, R^2 TOA and ATM (>1.96 = significant)

Secchi-disk transparency / **Landsat 7 ETM+ scenes**	**Samples**	**Eq1 & Eq2 TOA**	**Eq1 & Eq2 ATM**	**Eq 1 TOA & ATM**	**Eq 2 TOA & ATM**
path 20, row 30	15	1.199	†	†	†
path 20, row 31	13	1.637	†	†	†
path 21, row 29	28	1.233	1.212	0.065	0.086
path 21, row 30	29	.043	.043	.000	.000
path 21, row 31	25	.032	.022	.032	.043

Results

Comparison of Top of Atmosphere Reflection and Atmospheric-Correction Using Secchi-Disk Transparency

An initial expectation for this project was that use of atmospherically corrected images would produce higher R^2 values than use of the radiometrically corrected images. However, the R^2 results were not significantly different. In some cases, the atmospheric-correction produced slightly higher R^2 values than the radiometric-correction and in others produced slightly lower R^2 values (these differences in the R^2 values were only in the hundredths).

When Fisher's Transformation was used to test for the difference between R^2 values for the atmospherically corrected imagery and R^2 values for the radiometrically corrected imagery (tested on the R^2 values resulting from both regression equations), the values for each scene ranged between 0.000 and 0.086. Therefore, imagery atmospherically corrected by use of MODTRAN4 did not produce a better-fit equation or statistically higher R^2 values than did the radiometrically corrected imagery. The result from this test was that atmospherically corrected imagery was not necessary, and that radiometrically corrected imagery would be used to compute TSI values in this report. The R^2 values from atmospherically corrected imagery or radiometrically corrected imagery for either regression equation are listed in table 3.

Prediction of Secchi-Disk Transparency by Use of Two Different Regression Equations

In comparison of results for the equation of Kloiber and others (2002),

$$ln(SDT) = a(band1/band3) + b(band1) + c, \quad (8)$$

and the alternative regression equation that was derived and tested during the project,

$$ln(SDT) = a(band1) + b(band2) + c(band3) + d, \quad (9)$$

the alternative regression equation produced a better-fit equation and returned higher R^2 values for four of the five scenes with very little difference in values for the fifth scene. Figure 3 shows the predicted and actual SDT for path 21, row 30, (which returned the highest R^2 value), and for path 21, row 31, (which produced the lowest R^2 value).

When Fisher's Transformation was used to test for differences between R^2 values for the alternative regression equation and R^2 values from the first equation (tested on the R^2 values resulting from the atmospherically corrected imagery, and the radiometrically corrected imagery), the values for each scene were between 0.022 and 1.637. For each scene, the alternative regression equation had a higher R^2 value, but the difference was not statistically significant (table 4). Because the alternative regression equation improved the R^2 values for most scenes, it was substantially used to predict SDT for computing TSI values for lakes within the imagery. The computed TSI values for all lakes within the satellite imagery are shown on figure 4.

Table 4. Stepwise regression trials and R^2 values to predict trophic state index from chlorophyll *a*.

[TM, Landsat ETM + band; R^2, R-squared; *, Landsat ETM+ satellite bands used for regression in each trial; --, Landsat ETM+ satellite bands not used]

Stepwise regression trials			
Trial 1	**Best coefficients**	**Trial 2**	**Best coefficients**
TM 1	--	TM 4 / TM 3	--
TM 2	*	TM 2 / TM 3	--
TM 3	*	TM 2 - TM 3	--
TM 4	--	TM 1 / TM 2	--
TM 5	--	TM 3 / TM 1	*
TM 7	*	R^2 value	0.6341
R^2 value	0.8101		
Trial 3	**Best coefficients**	**Trial 4**	**Best coefficients**
(TM 2 + TM 3) / TM 2	--	TM 2	--
$TM\ 2^2$	--	TM 3	*
$TM\ 3^2$	*	TM 7	*
(TM 1 + TM 2) / 2	--	TM 3 / TM 1	--
(TM 1 + TM 3) / 2	*	$TM\ 3^2$	--
TM 3 / TM 4	--	(TM 1 + TM 3) / 2	*
R^2 value	0.6592	R^2 value	0.8045

Predicting Water Quality by Relating Secchi-Disk Transparency and Chlorophyll *a* Measurements to Satellite Imagery for Michigan Inland Lakes, August 2002

By L.M. Fuller, S.S. Aichele, R.J. Minnerick

Abstract

Inland lakes are an important economic and environmental resource for Michigan. The U.S. Geological Survey and the Michigan Department of Environmental Quality have been cooperatively monitoring the quality of selected lakes in Michigan through the Lake Water Quality Assessment program. Through this program, approximately 730 of Michigan's 11,000 inland lakes will be monitored once during this 15-year study. Targeted lakes will be sampled during spring turnover and again in late summer to characterize water quality. Because more extensive and more frequent sampling is not economically feasible in the Lake Water Quality Assessment program, the U.S. Geological Survey and Michigan Department of Environmental Quality investigate the use of satellite imagery as a means of estimating water quality in unsampled lakes. Satellite imagery has been successfully used in Minnesota, Wisconsin, and elsewhere to compute the trophic state of inland lakes from predicted secchi-disk measurements. Previous attempts of this kind in Michigan resulted in a poorer fit between observed and predicted data than was found for Minnesota or Wisconsin. This study tested whether estimates could be improved by using atmospherically corrected satellite imagery, whether a more appropriate regression model could be obtained for Michigan, and whether chlorophyll *a* concentrations could be reliably predicted from satellite imagery in order to compute trophic state of inland lakes. Although the atmospheric-correction did not significantly improve estimates of lake-water quality, a new regression equation was identified that consistently yielded better results than an equation obtained from the literature. A stepwise regression was used to determine an equation that accurately predicts chlorophyll *a* concentrations in northern Lower Michigan.

Introduction

The State of Michigan has more than 11,000 inland lakes; approximately 3,500 of these lakes are greater than 25 acres in size. Nearly all of these lakes greater than 25 acres have developed communities with permanent residences or vacation homes. The general public has access to launches or beaches at about 1,300 lakes in Michigan. Recreational value, property values, and ecological value are all closely related to the quality of water in these inland lakes (Krysel and others, 2003). Tourism in Michigan, much of which involves recreation at inland lakes, accounts for nearly $15 billion of economic activity each year (Stynes, 2002). Thus, inland lakes are important economic and ecological resources to Michigan.

The U.S. Geological Survey (USGS) and the Michigan Department of Environmental Quality (MDEQ) have been cooperatively monitoring the quality of inland lakes in Michigan through the Lake Water Quality Assessment (LWQA) monitoring program funded by the Clean Michigan Initiative. Through this program, the USGS will sample approximately 730 lakes over 25 acres in size with public access during a 15-year period. The 730 lakes are grouped into 45 major watershed management units. In a given year, a set of 7 to 10 of the 45 major watershed management units is chosen for sampling and lakes to be sampled are randomly selected from this set. After 5 years, at least some lakes in each of the 45 major watershed management units will have been sampled. This 5-year rotation will continue until year 2015, when all targeted 730 lakes have been sampled once. In addition, each year the MDEQ will provide data from their Cooperative Lakes Monitoring Program (CLMP), which is a volunteer network monitoring more than 200 lakes. Data from those two sampling networks are used to characterize baseline water quality and compute trophic state of monitored inland lakes.

Measured water-quality characteristics of inland lakes are critical factors in determining their recreational use, habitat and species diversity, and the economic return from the tourism industry. The USGS and the MDEQ monitor many inland lakes, but it is not economically feasible to monitor the quality of all 11,000 inland lakes in Michigan by use of conventional sampling techniques. Knowledge of the biological productivity of unsampled inland lakes is needed to assist resource managers in their efforts to help protect and manage the quality in all of Michigan's inland lakes.

Satellite imagery has been successfully used in Minnesota (Olmanson and others, 2001), Wisconsin (Batzli, 2003), and elsewhere (Baban, 1993; Dekker and Peters, 1993; Mayo and others 1995; Giardino and others, 2001) to estimate water quality for unsampled inland lakes. In previous studies in Michigan (Nelson and others, 2002; Wianwang, 2002) researchers attempted to use existing models for relating satellite imagery to specific water-quality variables; however, they were unable to obtain as high a coefficient of determination (R^2), which indicates the strength of a statistical relation, as previous studies in Minnesota and Wisconsin. A better method to predict trophic characteristics from satellite imagery would increase the knowledge every year about more of Michigan's inland lakes.

Purpose and Scope

The purpose of this report is to describe the methods and techniques used to develop estimates of Michigan lake-water quality on the basis of satellite images. Specifically, this report presents a brief overview of the conceptual basis for predicting trophic state on the basis of satellite images, describes methods used to develop a new alternative regression model for predicting secchi-disk transparency, and offers a new regression equation for predicting chlorophyll *a* concentrations in northern Lower Michigan. These two measures can further be used to estimate the trophic state of Michigan inland lakes.

Background

Naumann (1919) proposed a classification of lake-water quality ranging from oligotrophic (low phytoplankton populations and low primary productivity) to eutrophic (high phytoplankton populations and high primary productivity). Carlson (1977) proposed to quantify the trophic state by using a Trophic State Index (TSI), which can be used to group lakes into basic classes of oligotrophic, mesotrophic, eutrophic, and hypereutrophic. The natural progression of a lake from oligotrophic to eutrophic can be computed from measures of total phosphorus (TP), secchi-disk transparency (SDT), and chlorophyll *a* (Chl-*a*).

TP is measured directly by sampling and chemical analysis. SDT is a commonly used, low-cost technique that measures water clarity (Specifically, a black and white disk is lowered into the lake until it can no longer be seen). Water clarity is related to the quantity of phytoplankton in the water, although non-algal turbidity and tannic acids also can reduce water clarity. Chl-*a* measurements correlate with the concentration of phytoplankton within a given volume of lake water and are not affected by sediment or acids in the water. The formulas for computing TSI values are (Carlson, 1977):

$$TSI_{TP} = 14.41 * ln\ TP(milligrams\ per\ liter) + 4.15, \quad (1)$$

$$TSI_{SDT} = 60 - 14.41 * ln\ SDT(meters), \quad (2)$$

and

$$TSI_{CHL-a} = 9.81 * ln\ Chl-a(milligrams\ per\ liter) + 30.6 \cdot \quad (3)$$

The range of TSI values and how each measure is classified into oligotrophic, mesotrophic, eutrophic, and hypereutrophic is listed in table 1.

Typically, computing TSI values for a single lake using all three formulas should yield similar results. Increasing the phosphorus concentration generally results in increased phytoplankton concentration, which results in reduced water clarity. Yet at specific times of the year, results from the three formulas may not be congruous because of phosphorus nutrient uptake by macrophytes. Therefore, substantial amounts of macrophytes in a lake may alter the relation of the three TSI values. Of the three measures, SDT and Chl-*a* concentration have been quantified by use of satellite imagery techniques (Mayo and others, 1995; Zilioli and Brivio, 1997; Cox and others, 1998; Kloiber and others, 2000; Giardino and others, 2001; Kloiber and others, 2002).

Table 1. Lake trophic states and classification ranges for trophic state index, total phosphorus, secchi-disk transparency, and chlorophyll *a*.

[Based on Michigan Department of Environmental Quality report (1982) and modified by the State of Michigan to account for regional characteristics. TSI, Trophic State Index; SDT, secchi-disk transparency; Chl-*a*, Chlorophyll *a*; TP, Total Phosphorus; ft, feet; µg/L, micrograms per liter]

Lake trophic condition	Carlson TSI	SDT (ft)	Chl-*a* (µg/L)	TP (µg/L)
Oligotrophic	<38	>15	<2.2	<10
Mesotrophic	38–48	7.5–15	2.2–6	10–20
Eutrophic	49–61	3–7.4	6.1–22	20.1–50
Hypereutrophic	>61	<3	>22	>50

Satellites have been used to predict water characteristics since the 1970s. For example, the National Aeronautics Space Administration (NASA) Earth Resources Technology Satellite (ERTS-1) was used to determine an algal bloom in Lake Erie in 1972 (Strong, 1974). NASA's Landsat satellite series improved the spatial, spectral, and radiometrical resolutions allowing more water-quality parameters to be studied. The idea to relate SDT to satellite imagery started in the late 1970s and studies involving Chl-*a*, turbidity, and other water-quality characteristics soon followed (Scarpace and others, 1979; Lillesand and others, 1983; Verdin, 1985; Lathrop and Lillesand, 1986; Dekker and Peters, 1993; Mayo and others, 1995; Zilioli and Brivio, 1997). Landsat bands 1 through 4 signifying the visible and near infrared portions of the electromagnetic spectrum, were found to correlate well with water-quality characteristics (Lathrop and Lillesand, 1986). However, Lathrop (1992) found it difficult to use the same regression equation to characterize the water quality of different lakes. Recent studies found that, with improved methods, it was possible to predict water quality for unsampled lakes by use of regression equations relating existing measurements to remotely sensed data (Pulliainen and others, 2001; Kloiber and others, 2002; Thiemann and Kaufmann, 2002). These most recent studies form the basis for this project.

Imagery used in this study was collected by the Landsat 7 Enhanced Thematic Mapper Plus (ETM+) satellite launched in 1999 by NASA. The satellite orbits at an altitude of approximately 705 km with a sun-synchronous 98-degree inclination and a descending equatorial crossing time of 10:00 a.m. (Williams, 2003). Every 16 days, the satellite will repeat coverage for each scene coinciding with the Landsat Worldwide Reference System (WRS), which records satellite scenes into a grid reference system made up of 233 paths and 248 rows. The Landsat 7 ETM+ sensor collects information in nine bands, distinct portions of the electromagnetic spectrum. Bands 1, 2, 3, 4, and 8 are sensed within a spectral range between 0.4 and 1 µm. Bands 1, 2, and 3 correspond to the visible spectrum of blue, green, and red, and band 4 is infrared; together, these bands span the spectral range of 0.45 to 0.90 µm. Bands 5 and 7 are short-wavelength infrared bands sensed within a spectral range between 1 and 3 µm. Bands 6a and 6b are thermal long wavelengths sensed within a spectral range between 8 and 12 µm. Band 8 is the panchromatic band that combines bands 2, 3, and 4 with a spectral range of 0.52 to 0.90 µm (Williams, 2003). Data are reported in digital numbers as 8-bit integers, ranging from 1 to 256.

Several distortion factors affect satellite imagery. These factors include geometric distortions that are the result of small imprecisions in maneuvering the sensor; radiometric distortions that arise from small differences in the calibration of the sensor and geometry of the earth, sun, and satellite; and atmospheric distortions that arise from scattering of light by moisture and particulates in the atmosphere. However, procedures have been developed to help correct for these factors. Geometric and radiometric corrections can be made with little or no field data. However, most studies of this scope suggest that the imagery should be geometrically, radiometrically, and atmospherically corrected (Brivio and others, 2001; Zilioli and Brivio, 1997; Kloiber and others, 2002).

A variety of equations relating satellite imagery to STD have been tested in different settings and with different sensors. Researchers that use imagery from the Landsat 7 ETM+ satellite (Kloiber and others, 2002) have generally used the following equation:

$$ln(SDT) = a(band1/band3) + b(band1) + c . \quad (4)$$

The variables *a*, *b*, and *c* are empirically derived coefficients from the regression equation.

Nelson and others (2002) used raw digital numbers from the images and the regression equation identified in Kloiber and others (2002) to estimate SDT for lakes in Lower Michigan. Kloiber and others (2002) reported predictions with R^2 values between 0.72 and 0.93. Nelson and others (2002) achieved an R^2 of only 0.43 for Landsat ETM+ scenes in path 21, rows 29, 30, and 31. Wiangwang (2002) used the same imagery and field data as Nelson and others (2002) but radiometrically corrected the images before determining regression equations. This type of correction is termed "Top of Atmosphere" (TOA) reflectance because, although it accounts for differences in illumination angle and sensor performance, it does not adjust for haze or diffusion within the atmosphere. The R^2 value using SDT and Landsat 7 ETM+ TOA corrected imagery for path 21, rows 29, 30, and 31 was 0.558 (Wiangwong, 2002). This result suggests that a full atmospheric-correction of the imagery could in theory further improve the R^2 values. The combination of all of these techniques in the same case study should improve the regression equations, and thus lead to better methodology to estimate water quality from satellite imagery.

Study Area

The study area was determined by the location of LWQA sampling planned for the 2002 water year (the 2002 water year was a portion of the inland lakes chosen to be sampled from 10 out of the 45 basins in Michigan). Most measurements fell within five Landsat 7 ETM+ satellite scenes covering the majority of Lower Michigan. The locations of the satellite scenes and the lakes with collected SDT measurements within a window of plus or minus 7 days of the imagery acquisition, are shown in figure 1.

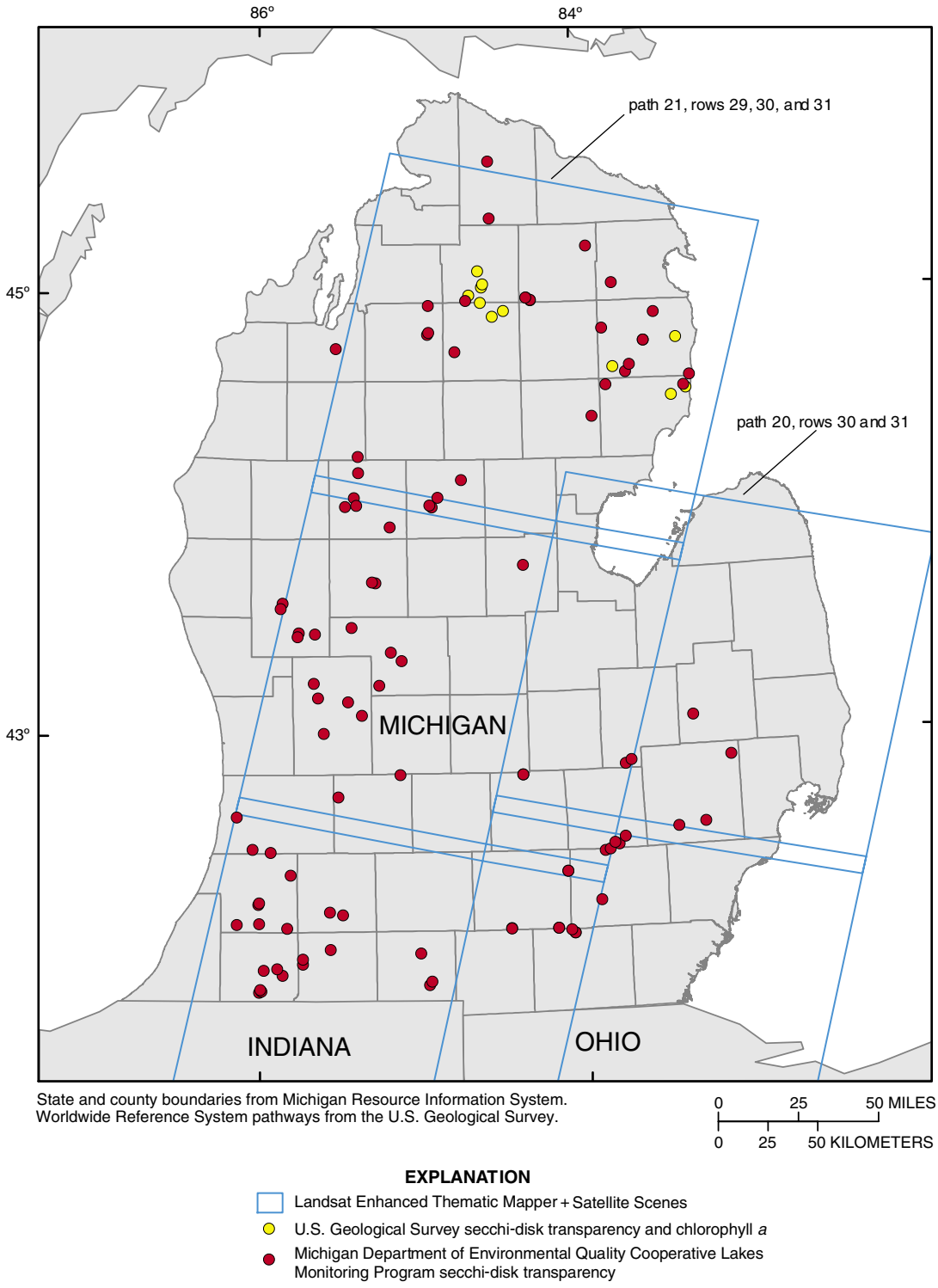

Figure 1. Secchi-disk transparency and chlorophyll *a* sample locations, Michigan, August 2002.

Methods

The general process to predict SDT and Chl-*a* measurements from satellite imagery involves several steps. First, field data must be obtained and digitized. Second, cloud-free satellite imagery from approximately the same date as the field data collection must be obtained. Third, the imagery must be corrected to compensate for geometric, radiometric, and atmospheric distortions in the imagery. Fourth, the field data must be compared to the imagery through the creation of Areas of Interest (AOI) within the satellite image. Fifth, a regression model must be developed for each scene to relate the field data to the spectral data collected in each AOI. Finally, the regression equation must be applied to all lakes over 25 acres in the satellite scene, to predict the water-quality characteristics at unmeasured locations.

Field Data Collection and Preprocessing

USGS scientists and community volunteers from the CLMP routinely measure SDT in various lakes in Michigan. A secchi disk is a common tool for measuring the overall clarity of water. The Secchi disk is an 8-in. diameter circular disk painted black and white in alternating quadrants. The disk is lowered into the water, and the depth at which the disk is no longer visible is called the secchi depth. Chl-*a*, TP, several forms of nitrogen, and major ions are also measured at USGS sample sites. Samples from both the CLMP and USGS were used from the months of August and September 2002. This late-summer index period, when a lake is at the maximum biological productivity, was found to be the best period for relating SDT and Chl-*a* samples to satellite imagery (Kloiber and others, 2000).

USGS measurements were referenced by coordinates obtained from the Global Positioning System (GPS) and were used to create a shapefile. A shapefile is the file format ArcGIS software uses to store the location, shape, and attribute information. The SDT measurements from CLMP were recorded on paper and did not include precise coordinates for the measurements; however, a bathymetric map for each lake marked in the approximate location for each measurement. With this information, another shapefile was made by manually digitizing the correct location for all data within the lakes.

Volunteer SDT measurements have been studied and proven to be comparable with those made by professionals (Canfield and others, 2002; Obrecht and others, 1998). However, careful consideration was involved in choosing which CLMP SDT measurements were used in this study. Only measurements that were clearly marked on attached bathymetric maps were digitized. Some volunteer data were excluded where multiple measurements were made in a single lake (only one measurement per lake was chosen within the deepest basin) and when the location of measurements could not be determined from the published bathymetric maps.

Only measurements collected within 7 days of an image acquisition date were used. This restriction was shown to produce the best results in predictive SDT models (Kloiber and others, 2002). The final exclusions for all measurements were dependent upon the satellite imagery. Measurements when clouds or cloud shadows covered the lake or measurement location were excluded. Clouds and shadows are limiting factors and are the reason imagery should be chosen on clear satellite overpass days. (For a summary of sample numbers per scene refer to table 4.)

Satellite Imagery Acquisition and Preprocessing

Five Landsat 7 ETM+ scenes were purchased from the Tropical Rain Forest Information Center, a member of NASA Federation of Earth Science Information Partners at the Center for Global Change and Earth Observations, Michigan State University. The scenes from path 20, rows 30 and 31, and path 21, rows 29, 30, and 31 were chosen because they had minimal cloud cover and were acquired closest to the dates when the measurements were collected. For reference, see figure 1, which depicts satellite scene locations with the placement of SDT and Chl-*a* measurements.

The data arrived with a geometric systematic correction, which helped ensure that the image cells would correspond to the data-collection points as closely as possible. The systematic correction refers to the type of geometric correction. “The end result is a geometrically rectified product free from distortions related to the sensor (e.g. jitter, view angle effects), satellite (e.g. attitude deviations from nominal), and earth (e.g. rotation, curvature)” (National Aeronautics Space Administration, 2003). However, the geometric correction did not use ground-control points to ensure complete geodetic accuracy, and NASA only claimed residual error to 250 m in flat terrain at sea level. When each image was compared with the Michigan transportation framework developed by the Michigan Center for Geographic Information, however, it was found to be accurate to within 2 cells, or about 60 m.

The satellite imagery was also radiometrically corrected by use of a radiative transfer model. Radiometric corrections are needed because the brightness of each pixel in a satellite image is “affected by sun angle, atmospheric interference, changes in detector response, and numerous other factors” (Kloiber and others, 2002). The atmospheric-correction method used was MODTRAN4, released by the Air Force Research Lab, Space Vehicles Directorate, in March 1999. This model is an atmospheric radiative transfer code and algorithm (Hoke, 1999).

Atmospheric-Correction

To test whether atmospherically correcting the imagery would achieve better fit regression equations, path 21, rows 29, 30, and 31 were atmospherically corrected. The atmospheric correction model MODTRAN4 (Hoke, 1999) was used. Each

satellite scene was run seven times through the model, keeping all parameters constant for each scene except the surface percent reflectance, which started at 0.1 and increased to 0.7. The different surface percent reflectances were used to construct regression equations that accounted for atmospheric scattering of both incoming solar radiation and outgoing reflected radiation. The results were equations describing the relation between reflected radiation and radiation measured at the sensor. These equations were then applied to their corresponding bands to atmospherically correct the imagery. The inputs are listed in table 2. The output slope and intercept coefficients for each band were used in an Erdas IMAGINE model (Erdas Inc, 2001) to build the equations to compute atmospherically corrected images. The equations take into account that shorter wavelengths, such as band 1, scatter more than longer wavelengths, such as band 5. The values for all bands generally increase with this correction, but band 1 shows the most increase and band 5, the least. Typical change between the TOA reflectance values and the resulting atmospheric-correction values for Lake Lansing in Ingham County are shown in figure 2.

Table 2. MODTRAN4 atmospheric-correction parameters and input.

[km, kilometers]

Parameter	Input
Surface percent reflectance	0.1 to 0.7
Atmospheric model	Midlatitude summer
Aerosol model	Rural extinction (default visibility = 23 km)
Season	Spring-summer
Visibility	23 km
Day of year	Dependent upon satellite scene
Latitude and longitude	Varied depending on center of satellite scene
Greenwich mean time of image acquisition	1430

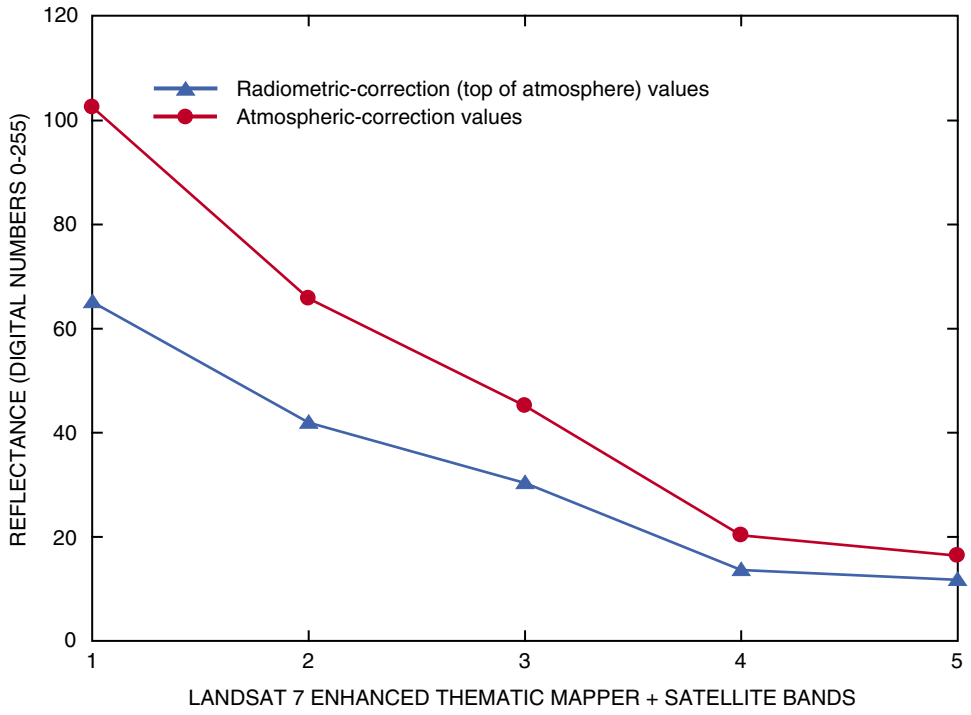

Figure 2. Radiometric-correction (top of atmosphere) reflectance values compared to atmospheric-correction values, Lake Lansing, Ingham County, Mich.

Relating Field Data to Satellite Imagery

Area of Interest Creation

The six shapefiles that were created corresponding to the SDT and Chl-*a* measurements for each scene were opened on top of the appropriate satellite scene in Erdas IMAGINE. Areas of Interest (AOIs) were digitized around the SDT measurements for five scenes, and Chl-*a* measurements for one scene. An area was drawn around each measurement to include pixels surrounding the measurements to help smooth radiometric noise. The AOI sizes depended on the size of the lake but were between the minimum of 8 pixels and the maximum of 1,000 pixels set by Olmanson and others (2001). The smallest AOI was 8 pixels, the mean was 12 pixels, and the maximum was 33 pixels.

Once all the AOIs were drawn around measurements within a satellite scene, each one was added to the signature file and the minimum, maximum, standard deviation, and mean value for each band within the AOI was computed. These results were then exported into a datafile format for further calculation. Results for the measurement values within the corresponding AOIs can be found in Appendix A.

Water-Only Imagery

A few steps were performed in Erdas IMAGINE to extract pixels in each image that would correspond to an inland lake greater than 25 acres. First, an unsupervised classification identified the water pixels (30-m cells). Next, the pixels were grouped into contiguous bodies of water to identify the inland lakes that were greater than 25 acres or 125 pixels. Finally, the pixels that corresponded to an inland lake greater than 25 acres were coded to a value of 1, with all other pixels coded to a no-data value to complete the water-only images.

Regression Equations and Tests of Significance for Secchi-Disk Transparency

In preparation for regression analysis, the band1/band3 ratio, the natural log of SDT (in meters) were computed. The data were then transferred into S-Plus 2000 (Data Analysis Products Division, 1999) for multiple regression calculations based on scene and type of measurement. (The combinations used in the regression equations are listed in table 3).

The equation developed by Kloiber and others (2000):

$$ln(SDT) = a(band1/band3) + b(band1) + c, \quad (5)$$

was applied to each TOA and atmospherically corrected scene. The variables *a*, *b*, and *c* were derived coefficients from the regression equation. In an effort to improve the goodness of fit for the model, various combinations of bands were tested. For the Kloiber (2000) equation, TOA and atmospherically corrected R^2 values were compared. A new, alternative equation also was developed during the project. For the new alternative equation,

$$ln(SDT) = a(band1) + b(band2) + c(band3) + d, \quad (6)$$

TOA and atmospherically corrected R^2 values were compared. To test whether there was a statistically significant difference between the R^2 values, Fisher's Transformation was used:

$$Z = (\{0.5*ln[(1+r_1)/(1-r_1)]\} - \{0.5*ln[(1+r_2)/(1-r_2)]\})/SQRT[1/(n-3)] \quad (7)$$

In the equation, r1 and r2 represent the two R^2 values that were being tested, ln refers to base *e* and *n* refers to the number of samples. The results of Fisher's Transformation had to surpass 1.96 for a 95-percent confidence interval. This test was also used to determine whether there was any difference between the two equations to compute TSI from the predicted natural log of SDT and to test whether there was any difference between using the TOA or atmospherically corrected scenes from path 21.

Stepwise Regression Equations for Chlorophyll *a*

To identify the best-fit regression equation for predicting Chl-*a*, a stepwise regression was used. In this process the natural log of measured Chl-*a* and various combinations of bands were used in four separate trials to determine the bands or combinations of bands with the best coefficients. For a list of the variables tested, refer to table 4.

Table 3. R^2 values and Fisher's Transformation significance tests used to compute trophic state index for Michigan's inland lakes from predicted secchi-disk transparency.

[ln, natural log; ETM+, Enhanced Thematic Mapper Plus; TOA, Radiometric-correction values of Top of Atmosphere Reflectance; ATM, Atmospheric-Correction; R^2, R Squared; Eq, equation; †, Not tested]

Equation 1	Independent variable: ln (secchi depth in meters)		
Secchi-disk transparency	**Dependent variables: band 1/band 3, and band 1**		
Landsat 7 ETM+ scenes	**Samples**	**TOA R^2**	**ATM R^2**
path 20, row 30	15	0.5075	†
path 20, row 31	13	.3003	†
path 21, row 29	28	.6640	0.6737
path 21, row 30	29	.7995	.7995
path 21, row 31	25	.6014	.6072

Equation 2	Independent variable: ln (secchi depth in meters)		
Secchi-disk transparency	**Dependent variables: band 1, band 2, band 3**		
Landsat 7 ETM+ scenes	**Samples**	**TOA R^2**	**ATM R^2**
path 20, row 30	15	0.7190	†
path 20, row 31	13	.6659	†
path 21, row 29	28	.7824	0.7875
path 21, row 30	29	.7964	.7964
path 21, row 31	25	.6058	.6101

Fisher's Transformation: R^2 Equation 1 and Equation 2, R^2 TOA and ATM (>1.96 = significant)

Secchi-disk transparency / **Landsat 7 ETM+ scenes**	**Samples**	**Eq1 & Eq2 TOA**	**Eq1 & Eq2 ATM**	**Eq 1 TOA & ATM**	**Eq 2 TOA & ATM**
path 20, row 30	15	1.199	†	†	†
path 20, row 31	13	1.637	†	†	†
path 21, row 29	28	1.233	1.212	0.065	0.086
path 21, row 30	29	.043	.043	.000	.000
path 21, row 31	25	.032	.022	.032	.043

Results

Comparison of Top of Atmosphere Reflection and Atmospheric-Correction Using Secchi-Disk Transparency

An initial expectation for this project was that use of atmospherically corrected images would produce higher R^2 values than use of the radiometrically corrected images. However, the R^2 results were not significantly different. In some cases, the atmospheric-correction produced slightly higher R^2 values than the radiometric-correction and in others produced slightly lower R^2 values (these differences in the R^2 values were only in the hundredths).

When Fisher's Transformation was used to test for the difference between R^2 values for the atmospherically corrected imagery and R^2 values for the radiometrically corrected imagery (tested on the R^2 values resulting from both regression equations), the values for each scene ranged between 0.000 and 0.086. Therefore, imagery atmospherically corrected by use of MODTRAN4 did not produce a better-fit equation or statistically higher R^2 values than did the radiometrically corrected imagery. The result from this test was that atmospherically corrected imagery was not necessary, and that radiometrically corrected imagery would be used to compute TSI values in this report. The R^2 values from atmospherically corrected imagery or radiometrically corrected imagery for either regression equation are listed in table 3.

Prediction of Secchi-Disk Transparency by Use of Two Different Regression Equations

In comparison of results for the equation of Kloiber and others (2002),

$$ln(SDT) = a(band1/band3) + b(band1) + c, \quad (8)$$

and the alternative regression equation that was derived and tested during the project,

$$ln(SDT) = a(band1) + b(band2) + c(band3) + d, \quad (9)$$

the alternative regression equation produced a better-fit equation and returned higher R^2 values for four of the five scenes with very little difference in values for the fifth scene. Figure 3 shows the predicted and actual SDT for path 21, row 30, (which returned the highest R^2 value), and for path 21, row 31, (which produced the lowest R^2 value).

When Fisher's Transformation was used to test for differences between R^2 values for the alternative regression equation and R^2 values from the first equation (tested on the R^2 values resulting from the atmospherically corrected imagery, and the radiometrically corrected imagery), the values for each scene were between 0.022 and 1.637. For each scene, the alternative regression equation had a higher R^2 value, but the difference was not statistically significant (table 4). Because the alternative regression equation improved the R^2 values for most scenes, it was substantially used to predict SDT for computing TSI values for lakes within the imagery. The computed TSI values for all lakes within the satellite imagery are shown on figure 4.

Table 4. Stepwise regression trials and R^2 values to predict trophic state index from chlorophyll *a*.

[TM, Landsat ETM + band; R^2, R-squared; *, Landsat ETM+ satellite bands used for regression in each trial; --, Landsat ETM+ satellite bands not used]

Stepwise regression trials			
Trial 1	**Best coefficients**	**Trial 2**	**Best coefficients**
TM 1	--	TM 4 / TM 3	--
TM 2	*	TM 2 / TM 3	--
TM 3	*	TM 2 - TM 3	--
TM 4	--	TM 1 / TM 2	--
TM 5	--	TM 3 / TM 1	*
TM 7	*	R^2 value	0.6341
R^2 value	0.8101		
Trial 3	**Best coefficients**	**Trial 4**	**Best coefficients**
(TM 2 + TM 3) / TM 2	--	TM 2	--
$TM\ 2^2$	--	TM 3	*
$TM\ 3^2$	*	TM 7	*
(TM 1 + TM 2) / 2	--	TM 3 / TM 1	--
(TM 1 + TM 3) / 2	*	$TM\ 3^2$	--
TM 3 / TM 4	--	(TM 1 + TM 3) / 2	*
R^2 value	0.6592	R^2 value	0.8045

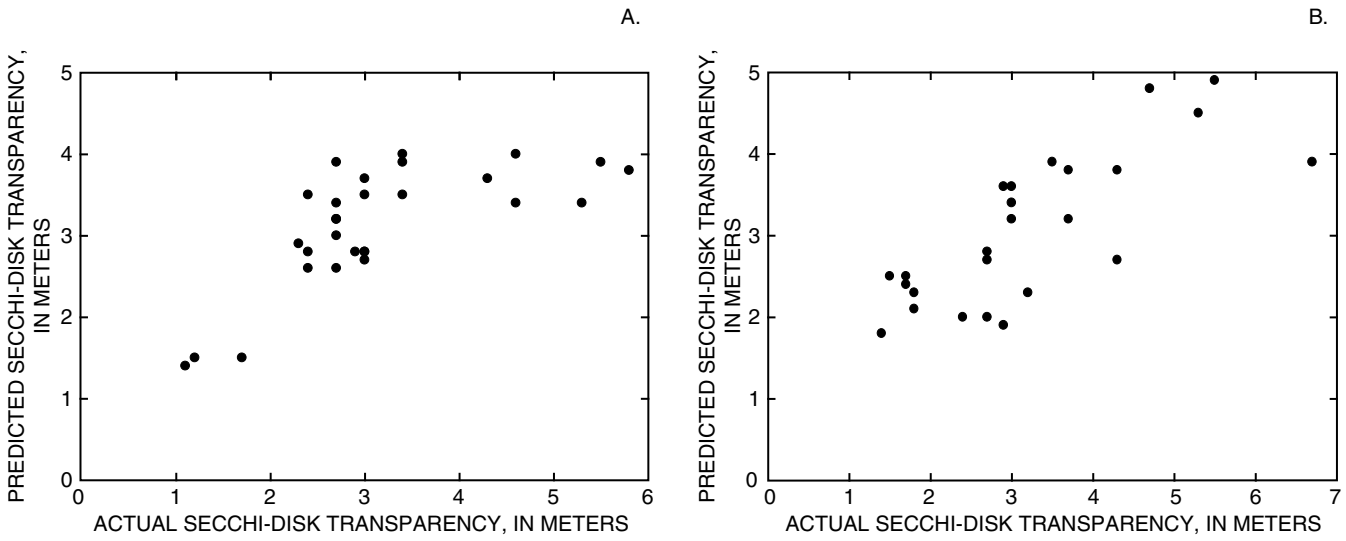

Figure 3. Predicted and actual secchi-disk transparency for (A) path 21, row 30, and (B) path 21, row 31.

Trophic State Index Computation from Predicted Chlorophyll *a* Measurements

In the stepwise regression used to identify an equation for relating the natural log of Chl-*a* to satellite imagery, the combination of band 2 (Green), band 3 (Red), and band 7 (short wave infrared) produced the highest R^2 values:

$$ln(Chl-a) = a(band2) + b(band3) + c(band7) + d. \quad (10)$$

The resulting R^2 value for predicting Chl-*a* measurements for path 21, row 29 was 0.81. Figure 5 shows predicted values and actual Chl-*a* values, figure 6 shows the computed TSI results from predicted Chl-*a*, and table 3 lists details of the stepwise regression variables and results.

Summary and Conclusions

The USGS and MDEQ have been cooperatively monitoring the quality of inland lakes in Michigan through the Lake Water Quality Assessment (LWQA) monitoring program funded by the Clean Michigan Initiative. The LWQA and MDEQ Cooperative Lakes Monitoring Program monitor water quality for selected inland lakes each year. Since Michigan has many inland lakes, it is impossible to physically collect the necessary data to compute TSI values for all inland lakes. Remote sensing is an effective and economical tool to enhance the value of conventional sampling data by producing regression equations to predict SDT and Chl-*a* measurements from satellite imagery. From these predictions of SDT and Chl-*a*, TSI values can be computed for most of Michigan's inland lakes.

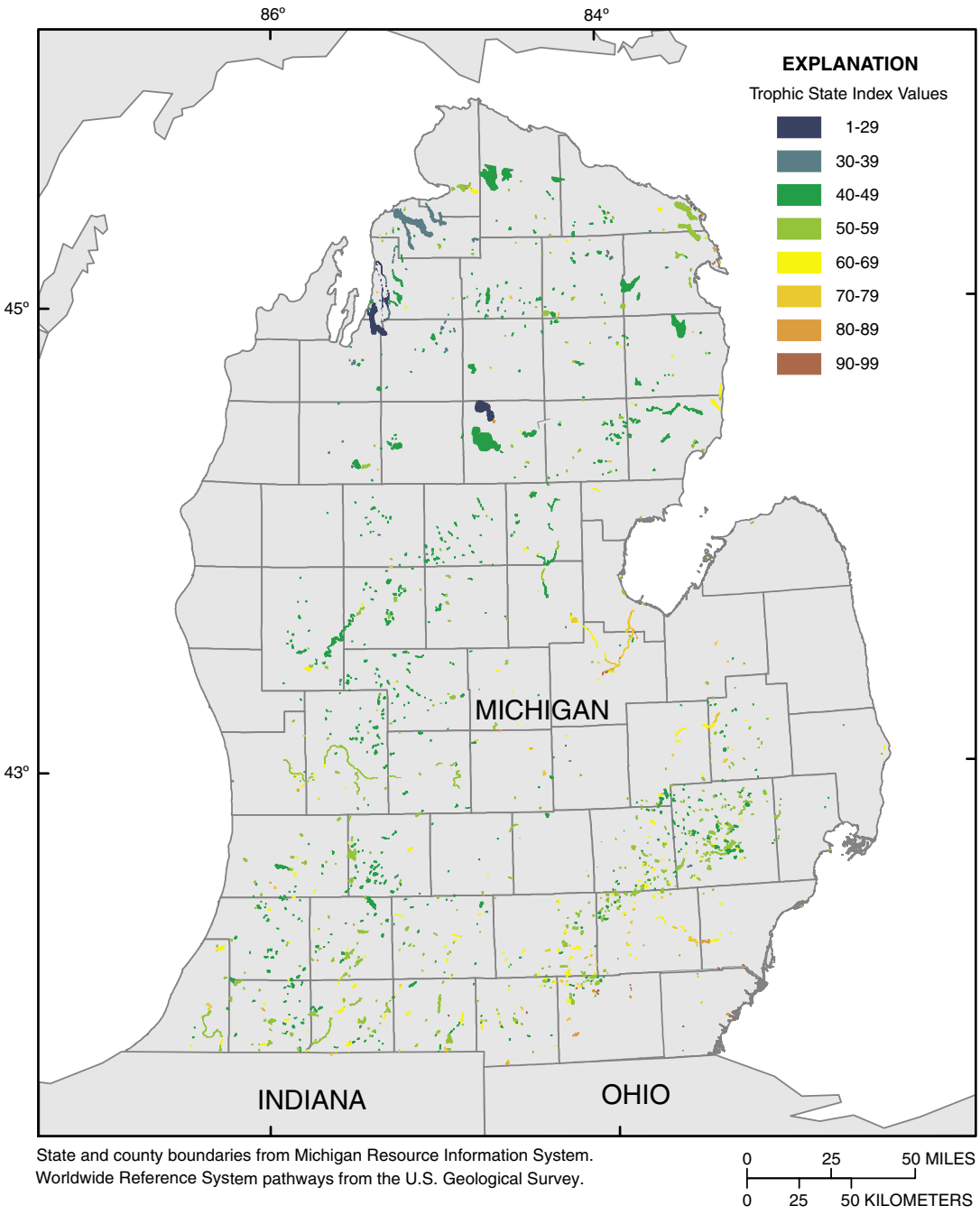

Figure 4. Computed trophic state index from predicted secchi-disk transparency, August 2002.

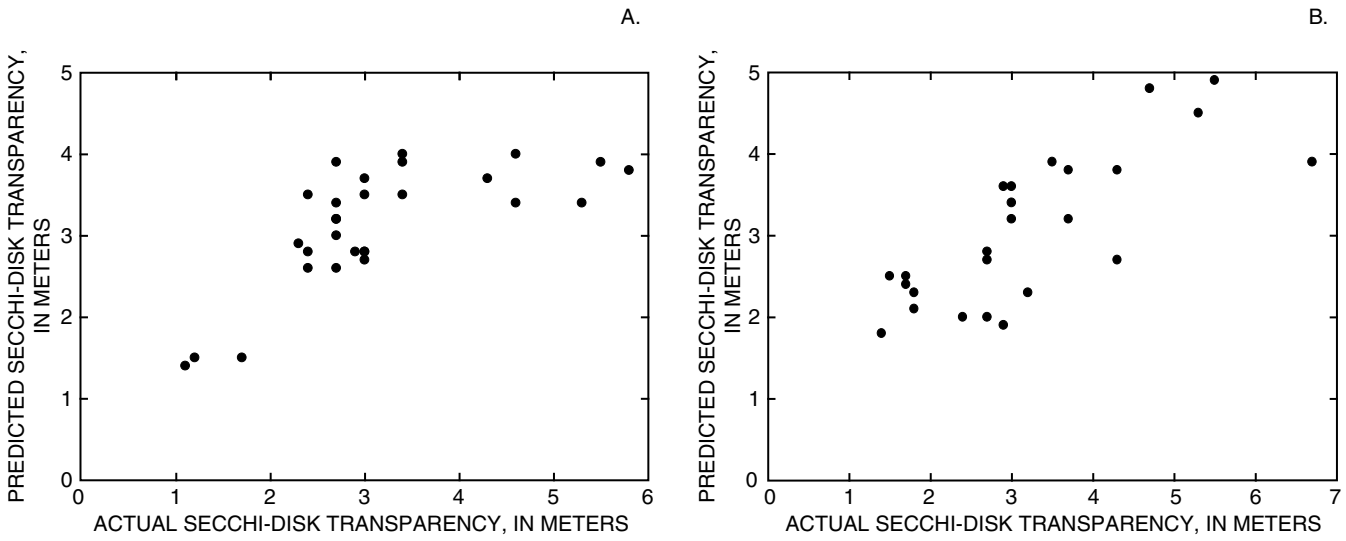

Figure 3. Predicted and actual secchi-disk transparency for (A) path 21, row 30, and (B) path 21, row 31.

Trophic State Index Computation from Predicted Chlorophyll *a* Measurements

In the stepwise regression used to identify an equation for relating the natural log of Chl-*a* to satellite imagery, the combination of band 2 (Green), band 3 (Red), and band 7 (short wave infrared) produced the highest R^2 values:

$$ln(Chl-a) = a(band2) + b(band3) + c(band7) + d. \quad (10)$$

The resulting R^2 value for predicting Chl-*a* measurements for path 21, row 29 was 0.81. Figure 5 shows predicted values and actual Chl-*a* values, figure 6 shows the computed TSI results from predicted Chl-*a*, and table 3 lists details of the stepwise regression variables and results.

Summary and Conclusions

The USGS and MDEQ have been cooperatively monitoring the quality of inland lakes in Michigan through the Lake Water Quality Assessment (LWQA) monitoring program funded by the Clean Michigan Initiative. The LWQA and MDEQ Cooperative Lakes Monitoring Program monitor water quality for selected inland lakes each year. Since Michigan has many inland lakes, it is impossible to physically collect the necessary data to compute TSI values for all inland lakes. Remote sensing is an effective and economical tool to enhance the value of conventional sampling data by producing regression equations to predict SDT and Chl-*a* measurements from satellite imagery. From these predictions of SDT and Chl-*a*, TSI values can be computed for most of Michigan's inland lakes.

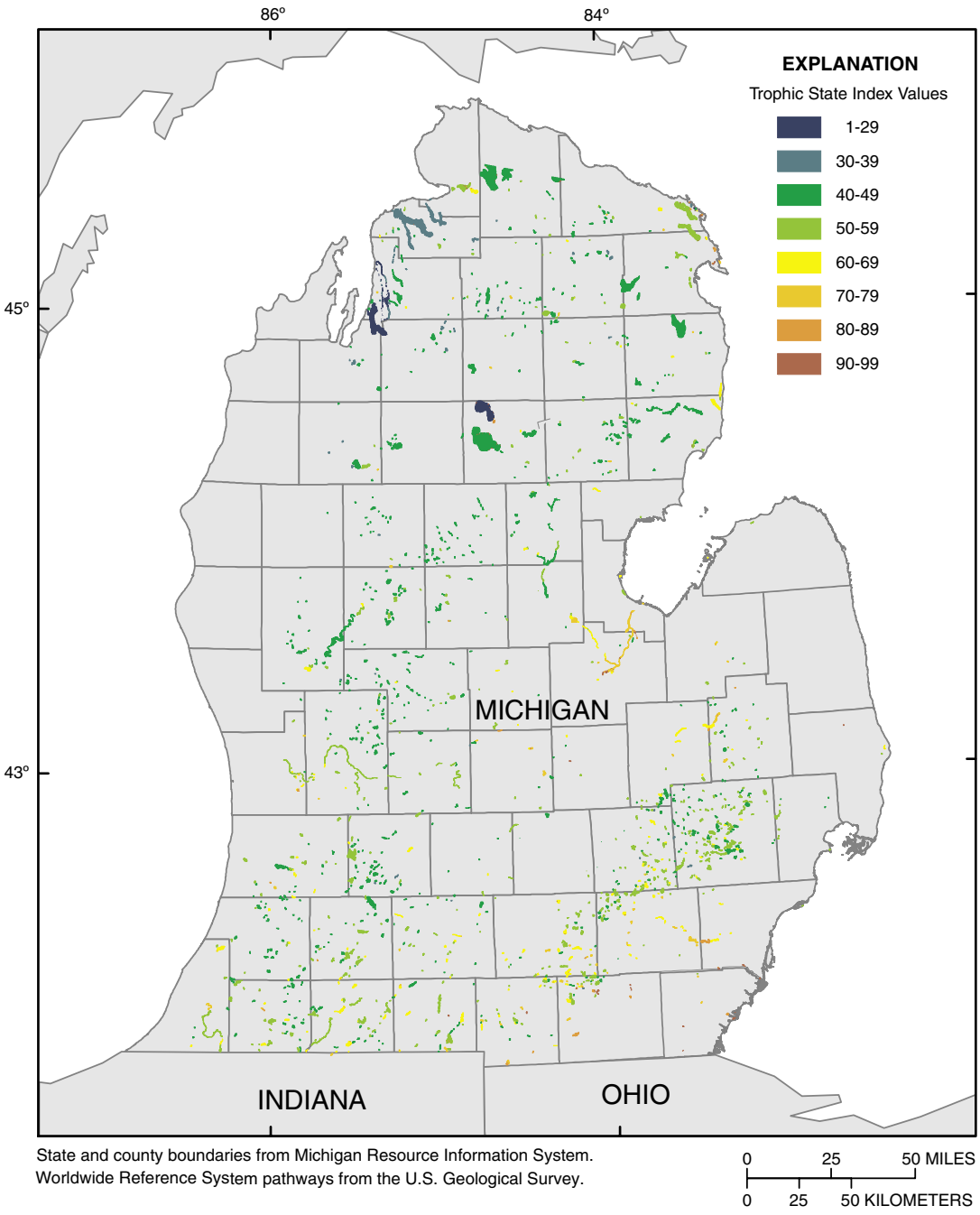

Figure 4. Computed trophic state index from predicted secchi-disk transparency, August 2002.

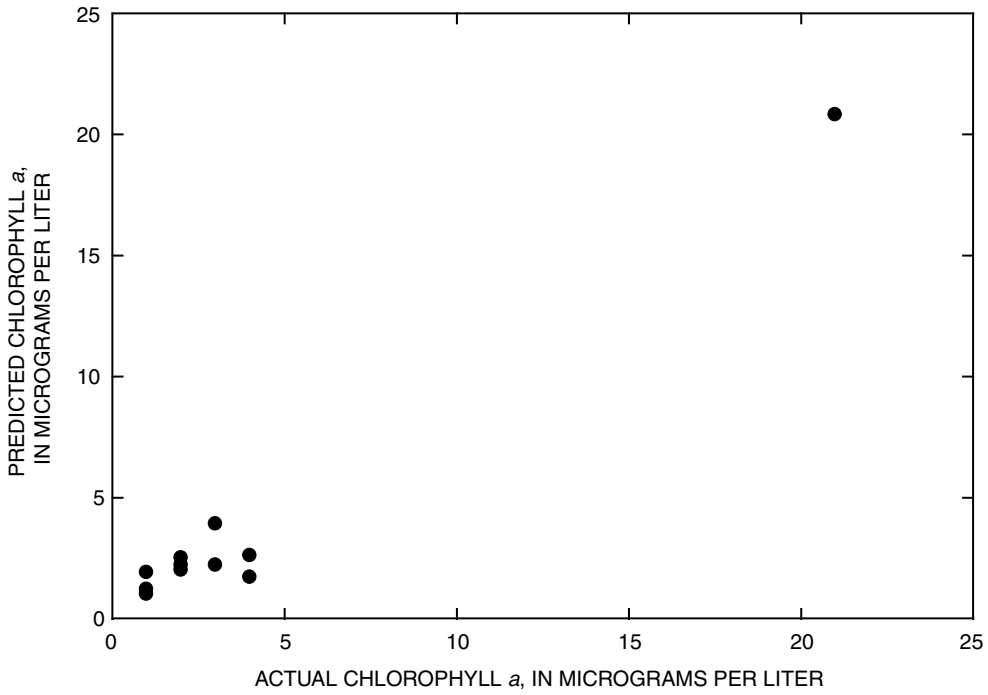

Figure 5. Predicted and actual chlorophyll *a* for path 21, row 29.

This study focused on 5 Landsat 7 ETM+ satellite scenes within Michigan, 87 SDT measurements, and 12 Chl-*a* measurements to find the best methods of predicting TSI values for inland lakes. As part of the study, atmospherically corrected images were tested against radiometrically corrected images to determine whether the atmospheric corrections would significantly improve the prediction of SDT. Differences between the R^2 values, for the two sets of images were small and not statistically significant.

A second part of the study was to test was whether an alternative regression equation would fit the SDT data better and produce higher R^2 values than a previously published equation from Kloiber and others (2000).

$$ln(SDT) = a(band1/band3) + b(band1) + c, \quad (8)$$

This equation produced R^2 values ranging from 0.30 to 0.80. An alternative equation was found to produce a better correlation and higher R^2 values ranging from 0.61 to 0.80.

$$ln(SDT) = a(band1) + b(band2) + c(band3) + d, \quad (9)$$

The improvement in R^2 values was not statistically significant but it was adopted for subsequent prediction of SDT on account of the higher R^2 values.

Finally, a stepwise regression was used to determine the best-fit equation between existing Chl-*a* measurements and various bands within the satellite imagery. This equation was developed for path 21, row 29 because that was the only scene with Chl-*a* measurements within plus or minus 7 days of the acquiring the imagery. The result of the stepwise regression was a regression equation that produced an R^2 value of 0.81.

$$ln(Chl-a) = a(band2) + b(band3) + c(band7) + d. \quad (10)$$

In addition to providing TSI estimates in unsampled lakes, remote-sensing techniques provide a cost-effective means of measuring both change through time and variability of water quality within a lake. Although TSI derived from satellite imagery is only an estimate of what the actual field sampled value might be, the cost per lake is dramatically lower compared to sampling. By using the high-quality measurements from the LWQA and CLMP programs, estimates can be made for entire Landsat scenes for approximately 10 percent the cost of field sampling. Operating both the field program and

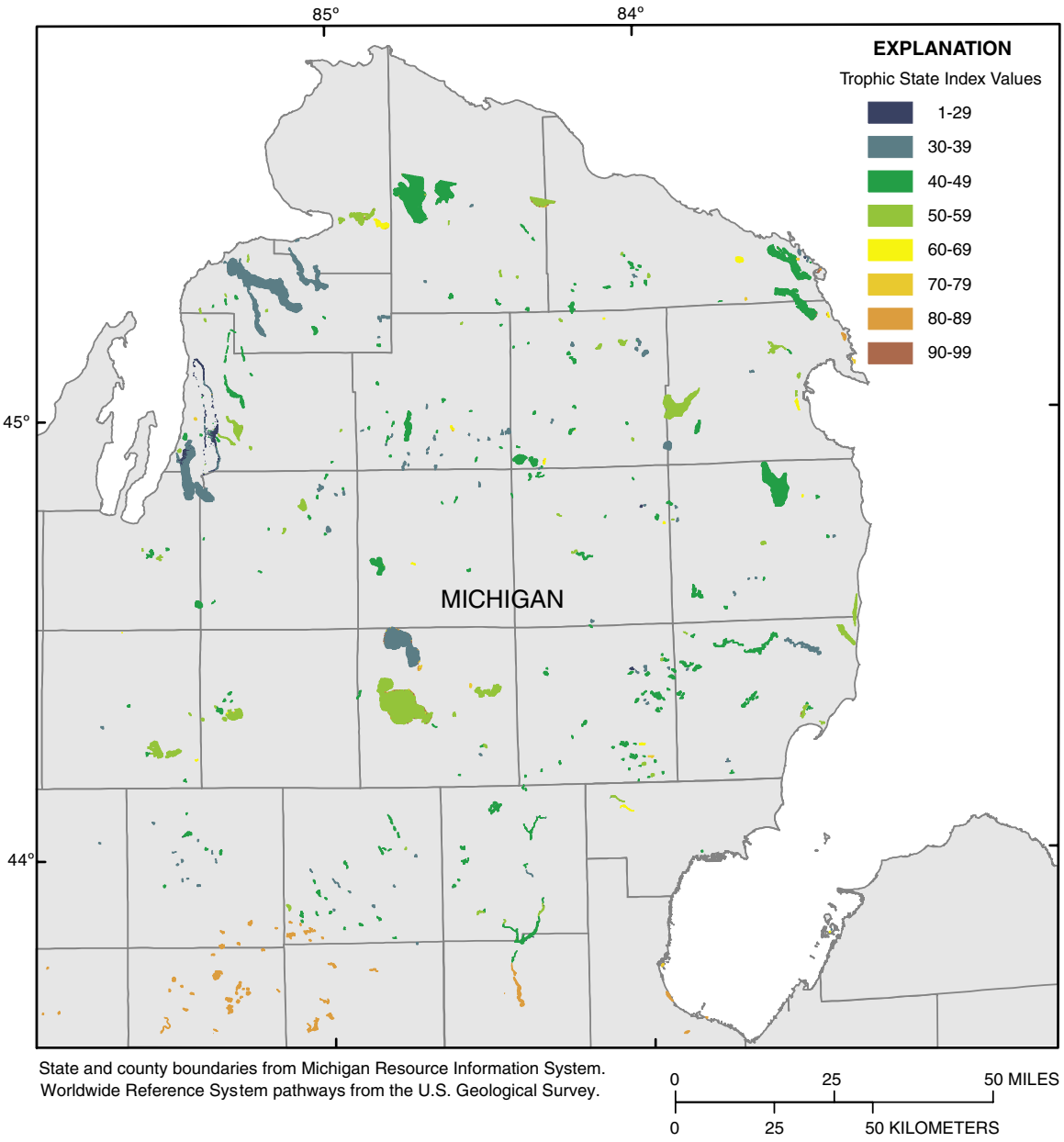

Figure 6. Computed trophic state index from predicted chlorophyll *a* for Landsat 7 ETM+ path 21, row 29, August 2002.

the remote sensing program will provide spatially continuous estimates of TSI for all lakes 25 acres or larger in size across Michigan, not just those selected for monitoring, and will increase temporal coverage because satellite-based estimates can be made for the same lakes on an annual or semiannual basis.

Acknowledgments

Mr. Ralph Bednarz of the Michigan Department of Environmental Quality and the volunteers of the Cooperative Lake Monitoring Program were invaluable in providing much of the field data used in the project. Dr. Jiagou Qi of the Michigan State University Department of Geography provided technical assistance with the atmospheric-correction process. Finally, Dr. Stacy Nelson, now at North Carolina State University, and Mrs. Naruman Wianwang of Michigan State University graciously provided assistance with this project.

References Cited

Baban, S.M.J., 1993, Detecting water quality parameters in the Norfolk Broads, UK, using Landsat imagery: International Journal of Remote Sensing, v. 14, no. 7, p. 1247–1267.

Batzli, S., 2003, Mapping lake clarity: About the map, accessed February 2003 at URL *http://www.lakesat.org/maptext1.php*

Booth, B., 2000, Getting started with ArcInfo 8: ESRI Incorporated, 230 p.

Brivio P.A., Giardino, C., and Zilioli, E., 2001, Validation of satellite data for quality assurance in lake monitoring applications: Science of the Total Environment, v. 268, p. 3–18.

Canfield, D.E., Brown, C.D., Bachmann, R.W., and Hoyer, M.V., 2002, Volunteer lake monitoring-testing the reliability of data collected by the Florida LAKEWATCH Program: Lake and Reservoir Management, v. 18, no. 1, p. 1–9.

Carlson, R.E., 1977, A trophic state index for lakes: Limnology and Oceanography, v. 22, p. 361–369.

Carpenter, D.J., and Carpenter, S.M., 1983, Modeling inland water quality using landsat data: Remote Sensing of Environment, v. 13, p. 345–352.

Cox, R.M., Forsythe, R.D., Vaughan, G.E., and Olmsted, L.L., 1998, Assessing water quality in Catawba River reservoirs using Landsat thematic mapper satellite data: Lake and Reservoir Management, v. 14, no. 4, p. 405–416.

Data Analysis Products Division, 1999, S-Plus 2000-modern statistics and advanced graphics: Seattle, Wash., Mathsoft, Inc., 868 p.

Dekker, A.G., and Peters, S.W.M., 1993, The use of the Thematic Mapper for the analysis of utrophic lakes–a case study in the Netherlands: International Journal of Remote Sensing, v. 4, no. 5, p. 799–821.

Erdas, Inc., 2001, Erdas IMAGINE-Tour guides: Atlanta, Ga., Erdas, Inc., 662 p.

Giardino, C., Pepe, M., Brivio, P.A., Ghezzi, P., and Zilioli, E., 2001, Detecting chlorophyll, secchi-disk depth and surface temperature in a sub-alpine lake using Landsat imagery: Science of the Total Environment, v. 268, p. 19–29.

Hoke, Mike, 1999, MODTRAN v4.0 r00 Software, accessed February 2003 at URL *http://www.vs.afrl.af.mil/Division/VSBYB/modtran4.html*

Kendall, M.G., 1951, The advanced theory of statistics, v. 2 (3d ed.): New York, Hafner Publishing Company, p. 116–117.

Kloiber, S.M., Anderle, T.H., Brezonik, P.L., Olmanson, L., Bauer, M.E., and Brown, D.A., 2000, Trophic state assessment of lakes in the Twin Cities (Minnesota, USA) region by satellite imagery: Archive Hydrobiologie Special Issues, Advances in Limnology, v. 55, p. 137–151.

Kloiber, S.M., Brezonik, P.L., Olmanson, L.G., and Bauer, M.E., 2002, A procedure for regional lake water clarity assessment using Landsat multispectral data: Remote Sensing of Environment, v. 82, p. 38–47.

Krysel, C., Boyer, E.M., Parson, C., and Welle, P., 2003, Evidence from property sales in the Mississippi Headwaters Region, accessed September 2003 at URL *http://info.bemidjistate.edu/News/currentnews/lakestudy/lakestudy.pdf*

Lathrop, R.G., 1992, Landsat Thematic Mapper monitoring of turbid inland water quality: Photogrammetric Engineering and Remote Sensing, v. 58, no. 4, p. 465–470.

Lathrop, R.G., and Lillesand, T.M., 1986, Use of Thematic Mapper data to assess water quality in Green Bay and Central Lake Michigan: Photogrammetric Engineering and Remote Sensing, v. 52, no. 5, p. 671–680.

Lillesand, T.M., Johnson, W.L., Deuell, R.L., Lindstrom, O.M., and Meisner, D.E., 1983, Use of Landsat data to predict the trophic state of Minnesota lakes: Photogrammetric Engineering and Remote Sensing, v. 49, no. 2, p. 219–229.

Mayo, M., Gitelson, A., Yacobi, Y.Z., and Ben-Avraham, Z., 1995, Chlorophyll distribution in Lake Kinneret determined from Landsat Thematic Mapper data: International Journal of Remote Sensing, v. 16, no. 1, p. 175–182.

Michigan Department of Natural Resources, 1982, Michigan Inland Lake Project-Identification, Survey and Classification: Lansing, Mich., Clean Lake Agreement No. S 005511-01.

National Aeronautics Space Administration, 2003, Chapter 11–Data products, Landsat 7 science data users handbook, accessed March 2003 at URL *http://ltpwww.gsfc.nasa.gov/IAS/handbook/handbook_htmls/chapter11/chapter11.html#section13*

Naumann, E., 1919, Some aspects of the ecology of the limnoplankton, with special reference to the phytoplankton: Svensk Botanisk Tidskrift, v. 13, no. 2, p. 129–163.

Nelson, S.A.C., Soranno, P.A., Cheruvelil, K.S., Batzli, S.A., and Skole, D.L., 2002, Assessing regional lake water clarity using Landsat and the role of inter-lake variability, accessed February 2003 at URL *http://foliage.geo.msu.edu/mdeq/docs/Nelson_RS-Secchi_text_2002__09.pdf*

Obrecht, D.V., Milanick, M., and Perkins, B.D., 1998, Evaluation of data generated from lake samples collected by volunteers: Lake and Reservoir Management, v. 14, no. 1, p. 21–27.

Olmanson, L.G., Kloiber, S.M., Bauer, M.E., and Brezonik, P.L., 2001, Image processing protocol for regional assessments of lake water quality: St. Paul, Minn., Water Resources Center and Remote Sensing Laboratory, University of Minnesota, p. 1–13.

Pulliainen, J., Kallio, K., Eloheimo, K., Koponen, S., Servomaa, H., Hannonen, T., Auriainen, S., and Allikainen, M., 2001, A semi-operative approach to lake water quality retrieval from remote sensing data: Science of the Total Environment, v. 268, p. 79–93.

Scarpace, F.L., Holmquist, K.W., and Fisher, L.T., 1979, Landsat analysis of lake quality: Photogrammetric Engineering and Remote Sensing, v. 45, no. 5, p. 623–633.

Strong, A.E., 1974, Remote sensing of algal blooms by aircraft and satellite in Lake Erie and Utah Lake: Remote Sensing of Environment, v. 3, p. 99–107.

Stynes, D.J., 2002, Michigan statewide tourism spending and economic impact estimates 1998-2000, accessed November 2003 at URL *http://www.prr.msu.edu/miteim/MichiganSatExec.pdf*

Thiemann, S., and Kaufmann, H., 2002, Lake water quality monitoring using hyperspectral airborne data–A semiempirical multisensor and multitemporal approach for the Mecklenburg Lake District, Germany: Remote Sensing of Environment, v. 81, p. 228–237.

Verdin, J.P., 1985, Monitoring water quality conditions in a large western reservoir with Landsat imagery: Photogrammetric Engineering and Remote Sensing, v. 51, no. 3, p. 343–353.

Wiangwang, N., 2002, Water clarity/trophic condition monitoring by using satellite remote sensing data: Michigan State University, Department of Geography Graduate Program, East Lansing, Mich., Masters paper.

Williams, D., 2003, The Landsat 7 Satellite, instrument and data, accessed February 2003 at URL *http://landsat.gsfc.nasa.gov/project/satellite.htm*l

Zilioli, E., and Brivio, P.A., 1997, The satellite derived optical information for the comparative assessment of lacustrine water quality: Science of the Total Environment, v. 196, p. 229–245.

APPENDIX A

Results and computations from the Areas of Interest created from the Landsat 7 Enhanced Thematic Mapper Plus satellite scenes in Lower Michigan by use of radiometrically corrected imagery and atmospherically corrected imagery

Appendix A. Results and computations from the Areas of Interest created from the Landsat 7 Enhanced Thematic Mapper Plus satellite scenes in Lower Michigan by use of radiometrically corrected imagery and atmospherically corrected imagery.

[Abbreviations: AOI, Area of Interest; ft, feet; m, meters; ln, natural log; SDT, secchi-disk transparency; TOA, radiometrically corrected top of atmosphere reflectance values; MDEQ, Michigan Department of Environmental Quality; CLMP, Cooperative Lakes Monitoring Program; ATM, atmospherically corrected values; Chl-*a*, chlorophyll-*a*; USGS, U.S. Geological Survey; µg/L, micrograms per liter; band values recorded in digital numbers (0–255)]

Satellite scene/ Lake name	AOI pixels	band 1	band 2	band 3	band 4	band 5	band 1/ band 3	SDT (ft)	SDT (m)	ln (SDT m)
path 20, row 30 TOA MDEQ CLMP										
Lake Nepessing	77	73.9870	48.8961	36.5325	17.4935	12.3507	2.0252	10.00	3.05	1.114
Baseline	57	65.5263	42.3509	31.0702	14.0526	11.3158	2.1090	11.50	3.51	1.254
Bass	37	69.3243	48.1351	33.0540	14.2432	11.6216	2.0973	9.83	3.00	1.097
East Crooked	50	67.0200	43.3600	31.7600	14.3400	11.9400	2.1102	10.00	3.05	1.114
West Crooked	26	66.0385	42.6154	31.7692	14.4231	11.8846	2.0787	6.50	1.98	.684
Ore	48	76.2500	58.8542	38.1250	14.5625	11.9167	2.0000	6.00	1.83	.604
Strawberry	33	68.7273	48.3636	34.9091	14.8182	11.7576	1.9688	6.17	1.88	.632
Zukey	24	75.0417	55.3750	37.2083	14.4583	11.8750	2.0168	8.34	2.54	.933
Green	26	71.8846	47.0000	32.9615	15.8462	12.3077	2.1809	14.00	4.27	1.451
Lakeville	37	73.1892	50.1892	36.8108	17.3243	12.2973	1.9883	12.00	3.66	1.297
Walled	48	70.5208	45.3750	32.9167	14.6250	11.9375	2.1424	17.75	5.41	1.688
White Lake	22	68.6818	43.2727	31.0454	15.0455	11.8182	2.2123	20.00	6.10	1.808
Byram	18	70.2778	48.8333	34.5556	16.0000	12.4444	2.0338	7.00	2.13	.758
Ponemah	29	69.1724	45.7241	34.2759	15.4483	11.9310	2.0181	8.17	2.49	.912
Lansing	88	78.8182	52.6818	40.4545	20.0909	13.6477	1.9483	10.00	3.05	1.114
path 20, row 30 ATM MDEQ CLMP										
Lake Nepessing	77	120.5974	79.5065	56.0779	26.9740	17.4026	2.1505	10.00	3.05	1.114
Baseline	57	106.5439	68.7895	47.8421	21.1404	16.1754	2.2270	11.50	3.51	1.254
Bass	37	112.7838	78.2162	50.8649	21.5405	16.5405	2.2173	9.83	3.00	1.097
East Crooked	50	109.0600	70.3000	48.9200	21.6800	16.9600	2.2294	10.00	3.05	1.114
West Crooked	26	107.4231	69.1539	48.8462	21.8846	16.8462	2.1992	6.50	1.98	.684
Ore	48	124.1875	95.5833	58.4583	22.1250	16.9375	2.1244	6.00	1.83	.604
Strawberry	33	111.9697	78.6364	53.5758	22.6364	16.7273	2.0899	6.17	1.88	.632
Zukey	24	122.3333	89.8750	57.0000	21.9167	16.7917	2.1462	8.34	2.54	.933
Green	26	117.1154	76.2692	50.6923	24.6923	17.3846	2.3103	14.00	4.27	1.451
Lakeville	37	119.3243	81.4865	56.4865	26.6757	17.3243	2.1124	12.00	3.66	1.297
Walled	48	114.8125	73.6250	50.5833	22.2500	16.9167	2.2698	17.75	5.41	1.688
White Lake	22	111.7727	70.0909	47.9545	23.0909	16.7727	2.3308	20.00	6.10	1.808
Byram	18	114.5000	79.5000	53.1111	25.0000	17.5000	2.1559	7.00	2.13	.758
Ponemah	29	112.5517	74.2414	52.5517	23.8966	16.9310	2.1417	8.17	2.49	.912
Lansing	88	128.4204	85.4773	62.0909	31.0114	19.2046	2.0683	10.00	3.05	1.114
path 20, row 31 TOA MDEQ CLMP										
Baseline	57	65.9649	42.7193	31.3684	14.1228	11.4561	2.1029	11.50	3.51	1.254
Bass	37	69.3784	48.2162	33.1351	14.2162	11.7297	2.0938	9.83	3.00	1.097
Coon	15	65.3333	41.5333	31.4667	15.2000	12.5333	2.0763	5.50	1.68	.517
East Crooked	50	67.0000	43.5200	31.8000	14.4400	11.9800	2.1069	10.00	3.05	1.114
West Crooked	26	66.3461	42.7692	31.7692	14.3077	11.8846	2.0884	6.50	1.98	.684
Ore	48	76.3125	58.7917	38.0417	14.5625	11.8542	2.0060	6.00	1.83	.604
Strawberry	33	69.0000	48.4545	35.2121	14.8788	11.7273	1.9595	6.17	1.88	.632
Zukey	24	75.0417	55.2917	36.9167	14.4583	11.8333	2.0327	8.34	2.54	.933

Appendix A. Results and computations from the Areas of Interest created from the Landsat 7 Enhanced Thematic Mapper Plus satellite scenes in Lower Michigan by use of radiometrically corrected imagery and atmospherically corrected imagery.—Continued

[Abbreviations: AOI, Area of Interest; ft, feet; m, meters; ln, natural log; SDT, secchi-disk transparency; TOA, radiometrically corrected top of atmosphere reflectance values; MDEQ, Michigan Department of Environmental Quality; CLMP, Cooperative Lakes Monitoring Program; ATM, atmospherically corrected values; Chl-*a*, chlorophyll-*a*; USGS, U.S. Geological Survey; µg/L, micrograms per liter; band values recorded in digital numbers (0–255)]

Satellite scene/ Lake name	AOI pixels	band 1	band 2	band 3	band 4	band 5	band 1/ band 3	SDT (ft)	SDT (m)	ln (SDT m)
path 20, row 31 TOA MDEQ CLMP--Continued										
Walled	48	70.4375	45.6042	33.3542	14.7917	11.9167	2.1118	17.75	5.41	1.688
Portage	82	65.7927	42.8902	30.5732	13.5488	11.2317	2.1520	13.40	4.08	1.407
Clear	59	67.7966	44.7458	31.2034	15.6441	12.1525	2.1727	9.00	2.74	1.009
Pleasant	24	66.6250	43.8750	32.3333	15.0000	12.0417	2.0606	7.08	2.16	.769
Vineyard	20	77.8000	52.6000	38.4000	18.7500	13.1000	2.0260	10.50	3.20	1.163
path 20, row 31 ATM MDEQ CLMP										
Baseline	57	109.6316	70.2807	48.3509	21.2807	16.3333	2.2674	11.50	3.51	1.254
Bass	37	114.8378	79.1081	50.9730	21.4595	16.6487	2.2529	9.83	3.00	1.097
Coon	15	108.6000	68.2667	48.4000	23.4000	17.6000	2.2438	5.50	1.68	.517
East Crooked	50	111.2400	71.5200	49.0400	21.8800	17.0200	2.2683	10.00	3.05	1.114
West Crooked	26	110.1539	70.3077	48.8846	21.6538	16.8462	2.2533	6.50	1.98	.684
Ore	48	126.4375	96.5000	58.3333	22.1250	16.8542	2.1675	6.00	1.83	.604
Strawberry	33	114.4242	79.4242	54.0303	22.7576	16.6667	2.1178	6.17	1.88	.632
Zukey	24	124.4583	90.7500	56.5833	21.9167	16.7500	2.1996	8.34	2.54	.933
Walled	48	116.7083	74.6458	51.2708	22.6250	16.8958	2.2763	17.75	5.41	1.688
Portage	82	109.2073	70.5122	47.0854	20.5122	16.0976	2.3194	13.40	4.08	1.407
Clear	59	112.4407	73.3729	48.0508	24.2034	17.1525	2.3400	9.00	2.74	1.009
Pleasant	24	110.7083	72.1667	49.8333	23.0000	17.0417	2.2216	7.08	2.16	.769
Vineyard	20	128.9500	86.2500	58.9500	28.7500	18.4000	2.1875	10.50	3.20	1.163
path 24, row 28 TOA USGS LWQA										
Arfelin	18	56.1667	33.5556	23.6111	12.1667	11.2778	2.3788	22.00	6.71	1.903
Witch	19	55.2105	33.1053	24.4737	12.1579	11.6316	2.2559	15.00	4.57	1.520
Horseshoe	16	54.3125	34.2500	24.3750	12.0000	11.0625	2.2282	8.00	2.44	.891
Keewaydin	17	54.1765	32.4706	23.6471	13.4706	11.4706	2.2910	9.00	2.74	1.009
Silver	10	54.4000	32.6000	24.7000	13.0000	11.7000	2.2024	10.00	3.05	1.114
Buck	18	54.9444	34.3889	24.2222	12.0000	11.1111	2.2683	8.00	2.44	.891
Indian	14	56.7857	35.7143	24.2143	11.8571	10.8571	2.3451	15.00	4.57	1.520
Emily	16	55.6250	34.5625	25.9375	12.0625	10.8750	2.1446	8.00	2.44	.891
Ottawa	21	56.9524	34.8571	23.8571	11.4762	10.4286	2.3872	19.00	5.79	1.756
path 24, row 28 ATM USGS LWQA										
Arfelin	18	91.3333	54.6111	36.2222	18.3333	16.1111	2.5215	22.00	6.71	1.903
Witch	19	89.6316	54.0000	37.4211	18.5263	16.5263	2.3952	15.00	4.57	1.520
Horseshoe	16	88.1875	55.6250	37.3125	18.3125	15.7500	2.3635	8.00	2.44	.891
Keewaydin	17	88.0000	52.8824	36.2941	20.5294	16.3529	2.4246	9.00	2.74	1.009
Silver	10	88.4000	52.9000	37.8000	19.8000	16.7000	2.3386	10.00	3.05	1.114
Buck	18	89.2778	55.8889	37.1667	18.1111	16.0000	2.4021	8.00	2.44	.891
Indian	14	92.1429	57.7857	37.0714	17.9286	15.6429	2.4855	15.00	4.57	1.520
Emily	16	90.3125	56.0000	39.5625	18.3125	15.6875	2.2828	8.00	2.44	.891
Ottawa	21	92.5714	56.5238	36.4286	17.4286	14.8571	2.5412	19.00	5.79	1.756
path 21, row 29 TOA USGS LWQA										
Brownlee	15	63.4667	41.6000	29.6000	13.4000	12.6000	2.1441	6.00	1.83	.604
Alcona Dam Pond	15	59.6000	37.4667	27.5333	13.5333	12.2667	2.1646	15.00	4.57	1.520
Jewell	11	64.7273	43.4545	31.2727	16.0909	13.5455	2.0698	11.00	3.35	1.210

Appendix A. Results and computations from the Areas of Interest created from the Landsat 7 Enhanced Thematic Mapper Plus satellite scenes in Lower Michigan by use of radiometrically corrected imagery and atmospherically corrected imagery.—Continued

[Abbreviations: AOI, Area of Interest; ft, feet; m, meters; ln, natural log; SDT, secchi-disk transparency; TOA, radiometrically corrected top of atmosphere reflectance values; MDEQ, Michigan Department of Environmental Quality; CLMP, Cooperative Lakes Monitoring Program; ATM, atmospherically corrected values; Chl-*a*, chlorophyll-*a*; USGS, U.S. Geological Survey; µg/L, micrograms per liter; band values recorded in digital numbers (0–255)]

Satellite scene/ Lake name	AOI pixels	band 1	band 2	band 3	band 4	band 5	band 1/ band 3	SDT (ft)	SDT (m)	ln (SDT m)
path 21, row 29 TOA USGS LWQA--Continued										
Van Etten	14	64.2857	46.7143	34.9286	13.9286	11.9286	1.8405	4.00	1.22	0.198
Foote Dam Pond	14	60.8571	36.5000	27.3571	12.7143	12.0714	2.2245	21.00	6.40	1.856
Shupac	19	63.1053	39.3158	27.0526	14.3158	11.9474	2.3327	26.00	7.92	2.070
West Twin	18	62.4444	40.3333	27.3333	12.8889	10.7778	2.2846	10.00	3.05	1.114
Dixon	12	64.6667	42.2500	28.1667	15.8333	12.7500	2.2959	16.00	4.88	1.584
Opal	9	63.8889	40.3333	27.0000	14.6667	12.0000	2.3663	12.00	3.66	1.297
K.P.	13	62.0000	38.8462	27.4615	14.3077	12.0000	2.2577	9.00	2.74	1.009
Emerald	12	59.5000	37.4167	26.3333	15.0000	12.3333	2.2595	11.00	3.35	1.210
Heart	12	63.3333	39.9167	27.4167	16.1667	12.7500	2.3100	22.00	6.71	1.903
path 21, row 29 ATM USGS LWQA										
Brownlee	15	101.2667	66.2000	44.7333	20.4000	17.5333	2.2638	6.00	1.83	.604
Alcona Dam Pond	15	95.0667	59.4000	41.6667	20.5333	17.2667	2.2816	15.00	4.57	1.520
Jewell	11	103.1818	69.0000	47.2727	24.3636	19.0909	2.1827	11.00	3.35	1.210
Van Etten	14	102.6429	74.2857	52.5714	21.0714	16.7143	1.9524	4.00	1.22	.198
Foote Dam Pond	14	97.1429	57.9286	41.3571	19.2143	16.7143	2.3489	21.00	6.40	1.856
Shupac	19	100.7368	62.5789	40.7895	21.6842	16.6842	2.4697	26.00	7.92	2.070
West Twin	18	99.7778	64.1667	41.3333	19.5556	14.9444	2.4140	10.00	3.05	1.114
Dixon	12	103.3333	67.0833	42.4167	23.9167	17.9167	2.4361	16.00	4.88	1.584
Opal	9	102.0000	64.3333	40.7778	22.2222	16.8889	2.5014	12.00	3.66	1.297
K.P.	13	99.0769	61.7692	41.5385	21.6154	16.7692	2.3852	9.00	2.74	1.009
Emerald	12	95.0000	59.3333	39.7500	22.8333	17.2500	2.3899	11.00	3.35	1.210
Heart	12	101.1667	63.5833	41.3333	24.5000	18.0000	2.4476	22.00	6.71	1.903
path 21, row 29 TOA MDEQ CLMP										
Vaughn	27	58.1852	35.2593	25.3704	14.9259	12.2593	2.2934	11.00	3.35	1.210
Jewell	22	64.6818	42.6818	30.7727	15.3636	13.5000	2.1019	9.00	2.74	1.009
Arnold	42	62.0476	38.5714	27.2619	14.7143	12.2143	2.2760	15.00	4.57	1.520
Lake Margrethe	91	64.5824	40.4725	27.6923	12.6154	11.0000	2.3321	12.00	3.66	1.297
Sage	42	58.7857	36.3333	25.9762	12.6190	11.1667	2.2631	12.50	3.81	1.338
North	21	59.7619	37.4286	26.7619	14.4286	12.4762	2.2331	14.00	4.27	1.451
Lake George	17	62.1765	39.2941	28.1765	16.0588	12.4706	2.2067	10.00	3.05	1.114
Shingle	15	62.4667	39.2000	28.8000	16.2667	13.2000	2.1690	11.00	3.35	1.210
Chain	12	58.3333	36.7500	25.9167	13.8333	12.3333	2.2508	12.00	3.66	1.297
Cub	21	65.2857	41.2381	27.8095	15.1905	12.2381	2.3476	19.00	5.79	1.756
Starvation	25	65.6800	40.4400	28.4000	15.7200	11.9600	2.3127	26.17	7.98	2.077
Avalon	109	67.6606	41.4495	26.7064	13.0917	10.9908	2.5335	25.00	7.62	2.031
East Twin	83	64.2892	42.5904	29.3012	13.1205	10.8554	2.1941	10.00	3.05	1.114
West Twin	38	62.4474	40.7105	27.3421	12.5789	10.8421	2.2839	11.00	3.35	1.210
Austin	16	63.6250	39.4375	28.5625	15.5000	12.5000	2.2276	10.00	3.05	1.114
Center	22	66.2273	41.0909	30.2727	18.2727	13.5909	2.1877	18.50	5.64	1.730
Wells	14	63.7857	39.7857	28.2857	15.6429	12.7143	2.2551	17.50	5.33	1.674
Stone Ledge	22	65.5455	42.2273	30.9545	16.0455	12.8182	2.1175	8.00	2.44	.891

Appendix A. Results and computations from the Areas of Interest created from the Landsat 7 Enhanced Thematic Mapper Plus satellite scenes in Lower Michigan by use of radiometrically corrected imagery and atmospherically corrected imagery.—Continued

[Abbreviations: AOI, Area of Interest; ft, feet; m, meters; ln, natural log; SDT, secchi-disk transparency; TOA, radiometrically corrected top of atmosphere reflectance values; MDEQ, Michigan Department of Environmental Quality; CLMP, Cooperative Lakes Monitoring Program; ATM, atmospherically corrected values; Chl-*a*, chlorophyll-*a*; USGS, U.S. Geological Survey; µg/L, micrograms per liter; band values recorded in digital numbers (0–255)]

Satellite scene/ Lake name	AOI pixels	band 1	band 2	band 3	band 4	band 5	band 1/ band 3	SDT (ft)	SDT (m)	ln (SDT m)
path 21, row 29 TOA MDEQ CLMP--Continued										
Beaver	57	65.2807	43.0000	29.1228	13.4912	11.3158	2.2416	10.00	3.05	1.114
Crooked	16	59.0000	37.0625	25.6875	13.7500	11.9375	2.2968	16.50	5.03	1.615
Hubbard	769	61.1534	38.5176	26.1222	11.0988	10.2263	2.3410	17.00	5.18	1.645
Cedar - Schmidt's Point	44	67.8182	51.6364	35.3864	11.8182	10.7045	1.9165	3.42	1.04	.042
Mullett - Red Pine Point	243	66.6872	43.0000	28.9959	12.0000	10.6049	2.2999	15.42	4.70	1.548
Wildwood	16	62.5625	39.1875	28.9375	14.1875	11.8750	2.1620	9.80	2.99	1.094
Lily	20	62.4500	38.3000	28.2000	14.7000	11.8000	2.2145	11.25	3.43	1.232
Bear	42	67.4762	40.8571	27.4048	14.0952	11.4286	2.4622	32.50	9.91	2.293
Indian	17	64.0000	39.8235	27.5294	16.1765	12.5882	2.3248	19.00	5.79	1.756
Big Bradford	28	62.8929	39.5714	26.7500	14.1786	11.9286	2.3511	16.00	4.88	1.584
path 21, row 29 ATM MDEQ CLMP										
Vaughn	27	93.0741	56.1111	38.3704	22.5926	17.0741	2.4257	11.00	3.35	1.210
Jewell	22	103.2273	67.8182	46.4091	23.3636	19.0455	2.2243	9.00	2.74	1.009
Arnold	42	99.1190	61.2857	41.1905	22.4048	17.0714	2.4064	15.00	4.57	1.520
Lake Margrethe	91	103.1319	64.4725	41.8462	19.1978	15.2857	2.4645	12.00	3.66	1.297
Sage	42	93.9762	57.8571	39.3095	19.1905	15.5000	2.3907	12.50	3.81	1.338
North	21	95.3333	59.4286	40.3333	22.0000	17.5714	2.3636	14.00	4.27	1.451
Lake George	17	99.2353	62.4706	42.5294	24.1176	17.4706	2.3333	10.00	3.05	1.114
Shingle	15	99.8000	62.2667	43.4000	24.5333	18.6000	2.2995	11.00	3.35	1.210
Chain	12	93.0833	58.4167	39.2500	21.0000	17.2500	2.3715	12.00	3.66	1.297
Cub	21	104.2381	65.6667	41.9048	23.0476	17.1905	2.4875	19.00	5.79	1.756
Starvation	25	104.7200	64.4800	42.8800	23.7600	16.7600	2.4422	26.17	7.98	2.077
Avalon	109	107.8624	65.9633	40.2385	20.0092	15.2294	2.6806	25.00	7.62	2.031
East Twin	83	102.6265	67.6024	44.1928	20.0723	15.0723	2.3222	10.00	3.05	1.114
West Twin	38	99.7105	64.8158	41.2368	19.1053	15.0000	2.4180	11.00	3.35	1.210
Austin	16	101.6250	62.8125	43.1875	23.5000	17.4375	2.3531	10.00	3.05	1.114
Center	22	105.5000	65.4545	45.7273	27.5909	19.1818	2.3072	18.50	5.64	1.730
Wells	14	101.9286	63.3571	42.7143	23.5714	17.6429	2.3863	17.50	5.33	1.674
Stone Ledge	22	104.6364	67.0455	46.7273	24.2273	17.9091	2.2393	8.00	2.44	.891
Beaver	57	104.1930	68.2632	43.9474	20.4211	15.6842	2.3709	10.00	3.05	1.114
Crooked	16	94.3125	58.8750	38.8125	20.8125	16.6875	2.4300	16.50	5.03	1.615
Hubbard	769	97.6112	61.1664	39.4421	16.9025	14.2471	2.4748	17.00	5.18	1.645
Cedar - Schmidt's Point	44	108.1136	82.2045	53.2955	17.9091	14.8182	2.0286	3.42	1.04	.042
Mullett - Red Pine Point	243	106.2798	68.2798	43.7407	18.2099	14.6914	2.4298	15.42	4.70	1.548
Wildwood	16	99.9375	62.2500	43.7500	21.4375	16.5625	2.2843	9.80	2.99	1.094
Lily	20	99.7000	60.7500	42.5500	22.4000	16.4000	2.3431	11.25	3.43	1.232
Bear	42	107.5952	65.0238	41.3810	21.2381	15.8571	2.6001	32.50	9.91	2.293
Indian	17	102.2941	63.4706	41.5882	24.4118	17.7059	2.4597	19.00	5.79	1.756
Big Bradford	28	100.4643	63.0000	40.3929	21.5000	16.7143	2.4872	16.00	4.88	1.584

Appendix A. Results and computations from the Areas of Interest created from the Landsat 7 Enhanced Thematic Mapper Plus satellite scenes in Lower Michigan by use of radiometrically corrected imagery and atmospherically corrected imagery.—Continued

[Abbreviations: AOI, Area of Interest; ft, feet; m, meters; ln, natural log; SDT, secchi-disk transparency; TOA, radiometrically corrected top of atmosphere reflectance values; MDEQ, Michigan Department of Environmental Quality; CLMP, Cooperative Lakes Monitoring Program; ATM, atmospherically corrected values; Chl-*a*, chlorophyll-*a*; USGS, U.S. Geological Survey; µg/L, micrograms per liter; band values recorded in digital numbers (0–255)]

Satellite scene/ Lake name	AOI pixels	band 1	band 2	band 3	band 4	band 5	band 1/ band 3	SDT (ft)	SDT (m)	ln (SDT m)
path 21, row 30 TOA MDEQ CLMP										
Lansing	50	65.1600	41.9600	30.3200	13.6200	11.7400	2.1491	10.00	3.05	1.114
Clear	29	64.5862	42.3448	30.3103	14.5172	12.9655	2.1308	9.00	2.74	1.009
Sanford	39	64.8974	40.5897	30.2821	14.8974	11.7692	2.1431	9.50	2.90	1.063
Lake George	16	62.1250	39.6250	27.7500	16.1875	12.3125	2.2387	10.00	3.05	1.114
Shingle	12	62.5833	39.0833	28.7500	16.0000	13.2500	2.1768	11.00	3.35	1.210
Bostwick	54	65.6852	43.8333	29.5741	13.2407	11.2593	2.2210	8.00	2.44	.891
Freska	12	61.9167	39.0000	27.5000	15.6667	12.5000	2.2515	9.00	2.74	1.009
Murray	30	65.1000	42.2667	29.4000	15.2000	12.1667	2.2143	7.50	2.29	.827
Reeds	43	68.0465	48.8605	33.4651	13.5814	11.2791	2.0334	4.10	1.25	.223
Derby	43	64.0698	39.9302	27.1860	14.0465	11.6977	2.3567	18.00	5.49	1.702
Brooks	31	66.8710	48.3871	34.0968	14.5161	11.5484	1.9612	3.50	1.07	.065
Hess	150	68.7667	54.0600	39.0333	13.4133	10.7133	1.7617	3.00	.91	-.089
Robinson	22	62.6818	38.3182	27.5000	14.0000	11.6818	2.2793	11.00	3.35	1.210
Austin	13	63.3077	39.5385	28.5385	15.5385	12.5385	2.2183	10.00	3.05	1.114
Big	43	65.5349	41.7907	30.0465	15.0698	11.7907	2.1811	9.83	3.00	1.097
Wells	13	63.7692	40.1538	28.3846	15.8462	12.5385	2.2466	17.50	5.33	1.674
Hutchins	38	64.8421	41.8947	28.8947	13.3947	11.6053	2.2441	9.00	2.74	1.009
Barlow	16	66.1250	43.0625	27.6875	13.9375	11.6250	2.3883	9.00	2.74	1.009
Jordan	38	65.6842	48.7895	33.1053	13.6579	11.2895	1.9841	5.50	1.68	.517
Lily	31	62.3226	38.4194	27.9032	14.6452	12.0000	2.2335	11.25	3.43	1.232
Camp	31	63.7419	39.4516	27.9032	13.9677	11.6452	2.2844	14.00	4.27	1.451
Blue	23	64.0435	42.0000	29.5217	13.6957	11.3913	2.1694	10.00	3.05	1.114
Round	23	63.9130	40.3043	29.0435	14.4348	12.1304	2.2006	9.00	2.74	1.009
Baldwin	9	63.4444	40.5556	27.8889	14.1111	11.7778	2.2749	8.00	2.44	.891
Clifford	18	62.6667	39.6111	28.6111	14.0000	11.7778	2.1903	15.00	4.57	1.520
Indian Lake	40	63.0250	39.6250	28.7250	14.0250	11.3750	2.1941	9.00	2.74	1.009
Bills	29	67.3793	44.4483	28.7241	13.5517	11.4138	2.3457	8.00	2.44	.891
Crystal	63	64.1429	39.1905	27.3016	13.9206	11.7302	2.3494	15.00	4.57	1.520
Indian	21	64.0000	39.9524	27.5238	16.4286	12.6190	2.3253	19.00	5.79	1.756
path 21, row 30 ATM MDEQ CLMP										
Lansing	50	102.5400	65.7800	45.1800	20.2800	16.3600	2.2696	10.00	3.05	1.114
Clear	29	101.6897	66.3103	45.2414	21.5172	17.9655	2.2477	9.00	2.74	1.009
Sanford	39	102.1795	63.6667	45.2051	22.0513	16.4359	2.2604	9.50	2.90	1.063
Lake George	16	97.8750	62.0000	41.3750	24.1875	17.2500	2.3656	10.00	3.05	1.114
Shingle	12	98.5833	61.3333	42.9167	23.9167	18.2500	2.2971	11.00	3.35	1.210
Bostwick	54	103.3148	68.7593	44.1667	19.5741	15.5741	2.3392	8.00	2.44	.891
Freska	12	97.5833	61.2500	40.9167	23.2500	17.3333	2.3849	9.00	2.74	1.009
Murray	30	102.4000	66.1000	43.9000	22.4333	17.0000	2.3326	7.50	2.29	.827
Reeds	43	107.1860	76.6047	50.0000	20.1628	15.6279	2.1437	4.10	1.25	.223
Derby	43	100.8837	62.6512	40.5581	20.9767	16.3256	2.4874	18.00	5.49	1.702

Appendix A. Results and computations from the Areas of Interest created from the Landsat 7 Enhanced Thematic Mapper Plus satellite scenes in Lower Michigan by use of radiometrically corrected imagery and atmospherically corrected imagery.—Continued

[Abbreviations: AOI, Area of Interest; ft, feet; m, meters; ln, natural log; SDT, secchi-disk transparency; TOA, radiometrically corrected top of atmosphere reflectance values; MDEQ, Michigan Department of Environmental Quality; CLMP, Cooperative Lakes Monitoring Program; ATM, atmospherically corrected values; Chl-*a*, chlorophyll-*a*; USGS, U.S. Geological Survey; µg/L, micrograms per liter; band values recorded in digital numbers (0–255)]

Satellite scene/ Lake name	AOI pixels	band 1	band 2	band 3	band 4	band 5	band 1/ band 3	SDT (ft)	SDT (m)	ln (SDT m)
path 21, row 30 ATM MDEQ CLMP--Continued										
Brooks	31	105.0968	75.8387	50.8710	21.5161	16.0323	2.0659	3.50	1.07	0.065
Hess	150	108.2933	84.8267	58.3133	19.8600	14.8000	1.8571	3.00	.91	-.089
Robinson	22	98.7273	60.0909	40.9545	20.8182	16.2273	2.4107	11.00	3.35	1.210
Austin	13	99.6923	62.0000	42.5385	23.0769	17.4615	2.3436	10.00	3.05	1.114
Big	43	103.0233	65.4419	44.8140	22.2791	16.4651	2.2989	9.83	3.00	1.097
Wells	13	100.3846	63.0000	42.1538	23.6154	17.3846	2.3814	17.50	5.33	1.674
Hutchins	38	102.0526	65.5526	43.1053	19.9211	16.2368	2.3675	9.00	2.74	1.009
Barlow	16	103.8750	67.3750	41.1875	20.8750	16.2500	2.5220	9.00	2.74	1.009
Jordan	38	103.3421	76.4474	49.3947	20.2368	15.6842	2.0922	5.50	1.68	.517
Lily	31	98.1613	60.3871	41.5806	21.6452	16.7097	2.3607	11.25	3.43	1.232
Camp	31	100.3871	61.9677	41.6452	20.7097	16.1613	2.4105	14.00	4.27	1.451
Blue	23	100.7391	65.7391	44.0435	20.4348	15.7826	2.2873	10.00	3.05	1.114
Round	23	100.5652	63.1739	43.2174	21.4348	16.9565	2.3270	9.00	2.74	1.009
Baldwin	9	99.8889	63.5556	41.6667	20.7778	16.4444	2.3973	8.00	2.44	.891
Clifford	18	98.6111	62.2222	42.6667	20.7778	16.3333	2.3112	15.00	4.57	1.520
Indian Lake	40	99.2750	62.1500	42.9000	20.7500	15.8500	2.3141	9.00	2.74	1.009
Bills	29	105.9655	69.7586	42.8276	20.0690	15.8276	2.4742	8.00	2.44	.891
Crystal	63	100.9683	61.5556	40.6508	20.6984	16.3651	2.4838	15.00	4.57	1.520
Indian	21	100.7143	62.7143	41.0000	24.4286	17.5714	2.4564	19.00	5.79	1.756
path 21, row 31 TOA MDEQ CLMP										
Randall	55	62.5636	42.0545	30.3091	13.8909	11.6000	2.0642	4.50	1.37	.316
Coldwater	124	63.9597	44.6210	30.1048	13.1774	12.2500	2.1246	6.00	1.83	.604
Birch	68	70.0441	45.0147	28.3824	14.3529	11.7353	2.4679	14.00	4.27	1.451
Diamond	95	66.9263	43.2737	28.2211	13.4842	11.2000	2.3715	10.00	3.05	1.114
Clear	56	64.5357	42.4464	30.1250	14.5000	12.9286	2.1423	9.00	2.74	1.009
Corey	93	67.2258	44.2258	28.3118	13.2043	11.1075	2.3745	9.50	2.90	1.063
Long	16	59.5625	38.5000	28.6250	14.6250	12.6250	2.0808	5.00	1.52	.421
Farwell	22	77.0909	54.6818	30.8636	14.8182	12.8636	2.4978	9.00	2.74	1.009
Vineyard	35	63.6286	43.8571	29.6286	13.4286	11.9143	2.1475	10.50	3.20	1.163
Indian	53	69.4151	50.4340	31.0943	13.2830	11.1509	2.2324	8.00	2.44	.891
Evans	32	59.2813	37.2188	26.0938	13.1250	11.9375	2.2719	18.00	5.49	1.702
Clear.0	46	63.0870	38.8913	27.3478	13.5000	11.7609	2.3068	11.50	3.51	1.254
Cedar	51	63.6667	38.8824	26.8039	13.0980	11.6667	2.3753	17.50	5.33	1.674
Fish	10	62.6000	39.8000	28.1000	14.9000	12.1000	2.2278	10.00	3.05	1.114
Lake of the Woods	39	63.0769	38.4872	27.3846	13.8974	11.6923	2.3034	12.00	3.66	1.297
Eagle	43	63.2326	38.7674	26.5349	13.4186	11.6047	2.3830	15.50	4.72	1.553
Hutchins	53	65.2830	41.6792	28.8868	13.4151	11.5094	2.2600	9.00	2.74	1.009
Osterhout	30	63.8333	39.8000	27.9333	14.4333	11.9000	2.2852	10.00	3.05	1.114
Christiana	53	64.5094	41.1698	29.3019	14.0189	11.4906	2.2015	5.50	1.68	.517
Juno	90	64.1778	40.2778	29.1111	14.2444	11.4000	2.2046	5.50	1.68	.517

Appendix A. Results and computations from the Areas of Interest created from the Landsat 7 Enhanced Thematic Mapper Plus satellite scenes in Lower Michigan by use of radiometrically corrected imagery and atmospherically corrected imagery.—Continued

[Abbreviations: AOI, Area of Interest; ft, feet; m, meters; ln, natural log; SDT, secchi-disk transparency; TOA, radiometrically corrected top of atmosphere reflectance values; MDEQ, Michigan Department of Environmental Quality; CLMP, Cooperative Lakes Monitoring Program; ATM, atmospherically corrected values; Chl-*a*, chlorophyll-*a*; USGS, U.S. Geological Survey; µg/L, micrograms per liter; band values recorded in digital numbers (0–255)]

Satellite scene/ Lake name	AOI pixels	band 1	band 2	band 3	band 4	band 5	band 1/ band 3	SDT (ft)	SDT (m)	ln (SDT m)
path 21, row 31 TOA MDEQ CLMP--Continued										
Painter	32	64.2813	39.8438	29.4063	14.8750	12.0313	2.1860	6.00	1.83	0.604
Gourdneck	40	63.1500	38.9750	28.0750	13.4000	11.2500	2.2493	12.00	3.66	1.297
Keeler	45	66.5778	43.2000	30.4444	14.6889	12.7111	2.1869	9.50	2.90	1.063
Reynolds (lower)	16	63.5625	40.3750	28.8125	15.5000	13.1250	2.2061	14.00	4.27	1.451
Reynolds (upper)	27	63.7407	39.5926	27.4444	13.5556	11.4815	2.3225	22.00	6.71	1.903
path 21, row 31 ATM MDEQ CLMP										
Randall	55	95.5455	64.3273	44.0909	19.9818	15.6727	2.1670	4.50	1.37	.316
Coldwater	124	97.6774	68.1532	43.7419	18.9677	16.6210	2.2330	6.00	1.83	.604
Birch	68	107.2941	68.7353	41.3382	20.7353	15.8382	2.5955	14.00	4.27	1.451
Diamond	95	102.2421	66.1368	41.0421	19.4526	15.0211	2.4912	10.00	3.05	1.114
Clear	56	98.6250	64.9464	43.8750	20.9821	17.5893	2.2479	9.00	2.74	1.009
Corey	93	102.7204	67.5806	41.2258	19.2043	14.9032	2.4917	9.50	2.90	1.063
Long	16	91.0625	58.8750	41.6250	21.1250	17.1875	2.1877	5.00	1.52	.421
Farwell	22	117.8182	83.8182	44.7273	21.5000	17.5000	2.6341	9.00	2.74	1.009
Vineyard	35	97.2286	67.0286	43.1429	19.4286	16.0857	2.2536	10.50	3.20	1.163
Indian	53	106.3019	77.0377	45.1321	19.2264	15.0189	2.3554	8.00	2.44	.891
Evans	32	90.6875	57.0938	37.9063	18.9688	16.0938	2.3924	18.00	5.49	1.702
Clear.0	46	96.4130	59.5652	39.7609	19.5217	15.8913	2.4248	11.50	3.51	1.254
Cedar	51	97.2157	59.5294	38.9020	18.8824	15.8039	2.4990	17.50	5.33	1.674
Fish	10	95.5000	60.9000	40.9000	21.7000	16.5000	2.3350	10.00	3.05	1.114
Lake of the Woods	39	96.4359	59.0513	39.8205	19.9231	15.6667	2.4218	12.00	3.66	1.297
Eagle	43	96.6047	59.4186	38.5581	19.4186	15.5814	2.5054	15.50	4.72	1.553
Hutchins	53	99.7358	63.8679	42.0566	19.4151	15.5094	2.3715	9.00	2.74	1.009
Osterhout	30	97.5333	60.9667	40.6333	20.8667	16.0333	2.4003	10.00	3.05	1.114
Christiana	53	98.4906	63.0189	42.6604	20.1509	15.4528	2.3087	5.50	1.68	.517
Juno	90	98.0667	61.6556	42.3889	20.5444	15.3778	2.3135	5.50	1.68	.517
Painter	32	98.1875	60.9375	42.7500	21.6563	16.2813	2.2968	6.00	1.83	.604
Gourdneck	40	96.4250	59.7250	40.8500	19.4000	15.0750	2.3605	12.00	3.66	1.297
Keeler	45	101.6889	66.0444	44.3333	21.3333	17.2889	2.2937	9.50	2.90	1.063
Reynolds (lower)	16	97.0000	61.7500	42.0000	22.5625	17.9375	2.3095	14.00	4.27	1.451
Reynolds (upper)	27	97.3333	60.6296	39.9259	19.5926	15.4444	2.4378	22.00	6.71	1.903

Appendix A. Results and computations from the Areas of Interest created from the Landsat 7 Enhanced Thematic Mapper Plus satellite scenes in Lower Michigan by use of radiometrically corrected imagery and atmospherically corrected imagery.—Continued

[Abbreviations: AOI, Area of Interest; ft, feet; m, meters; ln, natural log; SDT, secchi-disk transparency; TOA, radiometrically corrected top of atmosphere reflectance values; MDEQ, Michigan Department of Environmental Quality; CLMP, Cooperative Lakes Monitoring Program; ATM, atmospherically corrected values; Chl-*a*, chlorophyll-*a*; USGS, U.S. Geological Survey; µg/L, micrograms per liter; band values recorded in digital numbers (0–255)]

Satellite scene/ Lake name	AOI Pixels	band 1	band 2	band 3	band 4	band 5	band 7	Chl-*a* (µg/L)	ln (Chl-*a*)
path 21, row 29 USGS Chl-*a*									
Brownlee	13	62.92308	41.69231	29.69231	13.30769	12.69231	11.30769	3	1.10
Alcona Dam Pond	9	59.88889	37.66667	27.11111	13.77778	12.22222	11.11111	1	.00
Jewell	12	64.83333	43.41667	31.16667	16.08333	13.41667	11.66667	2	.69
Van Etten	10	64.30000	47.30000	35.20000	15.60000	12.30000	10.30000	21	3.04
Foote Dam Pond	13	61.30769	37.38462	26.92308	12.76923	12.38462	10.76923	2	.69
East Twin	18	65.16667	42.72222	28.77778	12.88889	11.00000	10.22222	4	1.39
Shupac	12	63.75000	39.50000	26.58333	14.50000	12.08333	11.00000	1	.00
West Twin	13	62.84615	41.69231	28.30769	12.84615	11.07692	9.76923	3	1.10
Dixion	14	65.71429	43.92857	29.21429	15.57143	12.85714	11.07143	1	.00
Opal	11	64.90909	42.00000	27.18182	14.63636	12.18182	10.36364	1	.00
Emerald	8	59.50000	37.37500	26.37500	14.87500	12.50000	10.87500	4	1.39
Heart	9	63.44444	40.22222	27.55556	16.11111	12.88889	10.55556	2	.69

Manuscript approved for publication, May 25, 2004
Prepared by the New Hampshire-Vermont District and Michigan District Publications Units—Debra H. Foster, Anita Cotton, Ann Marie Squillacci, and Sharon Baltusis (Michigan District)

For more information concerning the research in this report, contact:
Jim Nicholas, District Chief
U.S. Geological Survey
6520 Mercantile Way, Suite 5
Lansing, MI 48911-5991

or visit our Web site at:
http://mi.water.usgs.gov